

University of Windsor

Scholarship at UWindor

Electronic Theses and Dissertations

Theses, Dissertations, and Major Papers

1-1-1967

Liquid film flow-rate measurement at elevated pressures.

Kuldip Singh
University of Windsor

Follow this and additional works at: <https://scholar.uwindsor.ca/etd>

Recommended Citation

Singh, Kuldip, "Liquid film flow-rate measurement at elevated pressures." (1967). *Electronic Theses and Dissertations*. 6499.

<https://scholar.uwindsor.ca/etd/6499>

This online database contains the full-text of PhD dissertations and Masters' theses of University of Windsor students from 1954 forward. These documents are made available for personal study and research purposes only, in accordance with the Canadian Copyright Act and the Creative Commons license—CC BY-NC-ND (Attribution, Non-Commercial, No Derivative Works). Under this license, works must always be attributed to the copyright holder (original author), cannot be used for any commercial purposes, and may not be altered. Any other use would require the permission of the copyright holder. Students may inquire about withdrawing their dissertation and/or thesis from this database. For additional inquiries, please contact the repository administrator via email (scholarship@uwindsor.ca) or by telephone at 519-253-3000ext. 3208.

LIQUID FILM FLOW-RATE MEASUREMENT
AT ELEVATED PRESSURES

A Thesis
Submitted to the Faculty of Graduate Studies Through the
Department of Chemical Engineering in Partial Fulfilment
of the Requirements for the Degree of
Master of Applied Science at the
University of Windsor

by
Kuldip Singh

Windsor, Ontario
1967

UMI Number: EC52681

INFORMATION TO USERS

The quality of this reproduction is dependent upon the quality of the copy submitted. Broken or indistinct print, colored or poor quality illustrations and photographs, print bleed-through, substandard margins, and improper alignment can adversely affect reproduction.

In the unlikely event that the author did not send a complete manuscript and there are missing pages, these will be noted. Also, if unauthorized copyright material had to be removed, a note will indicate the deletion.

UMI[®]

UMI Microform EC52681

Copyright 2008 by ProQuest LLC.

All rights reserved. This microform edition is protected against unauthorized copying under Title 17, United States Code.

ProQuest LLC
789 E. Eisenhower Parkway
PO Box 1346
Ann Arbor, MI 48106-1346

ABL 1800

APPROVED BY:

Alex Gump

A. A. Nicol.

C. St. Pierre

168089

ABSTRACT

A knowledge of liquid film flow-rates is important for design purposes when accurate predictions are required of the conditions under which "dry out" heat flux occurs in nuclear-reactors and boilers. Liquid film flow-rates were measured for a steam-water mixture in cocurrent, upward, annular flow in a tube at pressures of 1,000 and 1,200 psia. Sinters located at the test section exit were used to extract the liquid film after the method of the Harwell group. Sinter lengths of 2-, 1- and 1/2-in. were employed to investigate the effect of length on the extracted liquid flow rates. The test section was a stainless steel pipe of inside diameter 0.493 in., approximately 200 diameters in length. The total mass flux ranged from $0.2 - 0.7 \times 10^6$ lbm/hr.ft² and the quality varied from 0.3 to 0.92.

The experimental film flow-rates were found to increase with decreasing mass flux and decreasing quality. Film flow-rates were consistently higher than the theoretical predictions using Levy's model with deviations as high as 64%. However, at the same total mass flux and quality, there was better agreement with Levy's model for the 1/2 in. sinter data. This suggests that the larger sinters may be extracting liquid from the main core. The experimental results

were also compared with predictions from Minh's model.
Deviations as large as +200% were obtained.

ACKNOWLEDGMENTS

The author wishes to express his gratitude and sincere appreciation to Dr. Carl C. St. Pierre for his guidance, criticism and encouragement throughout this work.

The experimental work for this thesis was performed at the Chalk River Nuclear Research Laboratories at the suggestion of Mr. E.O. Moeck. Special thanks is due to Mr. W.A. Crago who designed the test section used in the investigation and was closely associated with the author throughout the experimental work.

The financial support was provided by the National Research Council and Atomic Energy of Canada Ltd.

CONTENTS

ABSTRACT	iii
ACKNOWLEDGMENTS	v
TABLE OF CONTENTS	vi
LIST OF FIGURES	viii
LIST OF TABLES	x
I. INTRODUCTION	1
II. LITERATURE SURVEY	
A. Film Flow Rates	3
B. Pressure Drop	7
C. Equilibrium Flow Pattern	14
D. Models for Predicting Film Flow Rates	16
III. THEORY	
A. Slug-Annular Flow Transition	19
B. Liquid Film Flow Rate	22
IV. EXPERIMENTAL EQUIPMENT AND PROCEDURE	
A. Equipment	28
B. Measurement of Loop Variables	32
C. Experimental Procedure	35
V. RESULTS AND DISCUSSION	
Summary of Experimental Data	38
A. Pressure Drop	39
B. Liquid Film Flow Rates	43
C. Effect of Sinter Length	49
D. Comparison with Levy's Model	53
E. Comparison with Minh's Model	56
VI. CONCLUSIONS	58

NOMENCLATURE	60
REFERENCES	62
APPENDIX I	66
APPENDIX II	68
APPENDIX III	70
VITA AUCTORIS	72

FIGURES

<u>Figure</u>		<u>Page</u>
1	Typical Plot of Flow-Rate and Differential Pressure for High Exit Quality	25
2	Typical Plot of Flow-Rate and Differential Pressure for Low Exit Quality	26
3	Typical Plot of Steam Flow-Rate and Water Flow-Rate through the sinter	27
4	Schematic Diagram of the Loop	30
5	Test Section Details	31
6	Comparison of Owen's Model with Experimental Data ($f_{TP} = f_1$)	40
7	Comparison of Owen's Model with Experimental Data ($f_{TP} = \bar{f}$)	41
8	Comparison of Martinelli and Nelson Model with Experimental Data	42
9	Variation of Film Flow Rates with Quality for 2-inch sinter	44
10	Variation of Film Flow Rates with Quality for 1-inch sinter	45
11	Variation of Film Flow Rate with Quality for 1/2-inch sinter	46
12	Variation of Film Flow Rate with Mass Flux for 2-inch sinter	47
13	Flow Pattern Diagram Constructed from the Cine Film Results for Steam/Water Flow at 1000 psia	48
14	Variation of Film Flow Rates with Sinter Length	51

15	Comparison of Levy's Model with Experimental Data	54
16	Comparison of Minh's Model with Experimental Data	57

TABLES

<u>Table</u>		<u>Page</u>
4.1	Range of Experimental Parameters	37
5.1	Summary of Experimental Data	38
5.2	Relative Performance of Sinters	55

I. INTRODUCTION

For a number of years now, the phenomenon of critical heat flux* or "burnout" associated with two phase systems has received considerable attention from innumerable investigators. Although extensive investigations have been performed, the final answer to the nature of burnout has not yet been obtained. One of the important parameters related to the critical heat flux is the liquid film flow rate at the wall. This is especially true for high quality annular flow in which "dryout" of the liquid film near the wall leads to the flow boiling crisis.

The object of the present work was to measure the liquid film flow rate at elevated pressures by use of a sinter located at the exit of a test section. The effect of sinter length, pressure, total mass flux and quality on the film flow rate was studied. The test section employed was a 3/8 in, Sch 40, stainless steel pipe (I.D. 0.493 in). The length of the test section was about 200 diameters. This length is believed to be sufficient to allow for the distribution of the liquid in the gas phase and the liquid film to become constant.

*Critical heat flux is defined as the heat flux at which the rapid deterioration of the cooling process occurs.

Sinter lengths of 2-, 1- and 1/2-inch were used. The total mass flux was varied from 0.2 to 0.7×10^6 lbm/(hr. ft²) and steam quality ranged from 0.3 to 0.92. Runs were made at pressures of 1000 and 1200 psia. However, only limited data were obtained at a pressure of 1200 psia so that no generalized effects of pressure on film flow rate can be given at this time.

The experimental liquid film flow rates were compared with the theoretical models proposed recently by Levy (1) and Minh (2).

II. LITERATURE SURVEY

In order to better appreciate the work done here, a brief review is given of the various aspects of adiabatic, two-phase flow and the literature already available on this subject.

A. Film Flow Rates

Burn-out presents one of the principal limitations in the design of liquid or wet steam-cooled nuclear reactors, rocket nozzles and other high-specific-power equipment.

The measurement of liquid film flow rates is important in studying the phenomenon of burn-out or departure from nucleate boiling (DNB). In the past few years, a number of investigators (3-12) have studied the problem of burn-out in forced convection flow in order to gain a better understanding of the burnout mechanism. A knowledge of the factors affecting the burnout mechanism can possibly lead to methods of increasing the burnout limit. This can result in more economical boiling water reactors.

There is no certainty as to the dependence of the burnout heat flux in annular flow on the various system--describing parameters of a burnout experiment. The available theories for predicting burnout are based on three models: film dryout (3, 4, 5), film break-up (6) and droplet depletion (7). The droplet depletion model suggests that the controlling

mechanism for burnout in flowing systems is to be found in the eddy diffusion--limited transport of liquid droplets through a steam boundary layer to the heated wall. This model, however, was found to be inconsistent with experimental observations (8).

In the models based on film dryout, it is generally assumed that the liquid film on the wall steadily diminishes by the net effects of evaporation, entrainment and deposition until a dry patch occurs and the heater at that point becomes too hot to be rewetted. The first experiment confirming this was performed recently by Hewitt (3). Hewitt measured the quantity of water flowing on the inner heated tube of an annulus. Water was introduced in the form of a thin film through a porous sinter at the bottom of the heated rod. The water film was allowed to flow up under the action of steam which was introduced in the annular gap. The experiment enabled a direct observation of the burnout phenomenon in annular flow. Measurements of film flow rates showed that the burnout at high qualities corresponded closely with the point at which the film flow decreased to zero.

In another experiment by Staniforth (4), the film flow rate was measured at the end of a uniformly heated round tube using Freon-12 at 155 psia as the working fluid. In these experiments, the test section was supplied with a liquid phase only to test whether Hewitt's (3) conclusions apply equally well in such a situation. This experiment

also showed that the liquid film flow rate at the tube exit was reduced nearly to zero as the burnout heat flux was approached. It was not shown conclusively that burnout coincided with dryout of the liquid film on the heated wall but the film flow rate at burnout was so small that the assumption of zero film flow at burnout produces a very small error (8).

Hewitt (5) performed similar experiments with water as the working fluid at low pressures. The liquid film flow measurements substantiated the findings of the previous workers (3, 4) in relation to burnout heat flux and film flow rate. Burnout models based on film dryout and making use of film flow rate in one form or another were given by Isbin (9), Becker and Persson (10), Grace (11) and Grace and Isbin (12).

It has been shown experimentally (8) that if film instability followed by film break-up is the correct mechanism of burnout, it occurs at very small film flow rates so that film dryout and film instability models could be virtually indistinguishable. Both models will require for their numerical evaluation a means of calculating the amount of liquid flowing on the heated wall at any point in the channel. This film flow rate depends on the rate of droplet deposition, rate of entrainment of liquid from the film into the vapour core and initial flow distribution at the onset of annular flow.

An extensive review of various techniques for measurement

of liquid film flow rates has been given by Collier and Hewitt (13) in a recent paper. The first attempt to measure the liquid film flow rate by substituting a porous sinter was made by Gill and Hewitt (14). Their results were not very successful. Since then, a number of workers (3, 4, 5, 15) have successfully measured the film flow by employing a sinter in the following manner. The sinter, whose internal diameter is the same as that of the test section, is located at the exit of the test section. Care is taken to ensure that the bore is continuous and that there are no ridges at the various joints. This is felt to be essential since such ridges may disturb the liquid film on the surface. Suction is then applied on the outside of the sinter to remove the liquid film flowing along the tube wall. At operating pressures higher than atmospheric, no suction is required.

In all experiments of this type, each investigator used a different sinter length. Hewitt (3, 5) chose a sinter length of 0.5 in, Staniforth (4) employed a 2.5 in sinter and Cousins (15) used a 3 in length. It is not known if the length of the sinter had any effect on the measurement of liquid film flow rates. Too long a sinter may suck off excessive amount of droplets from the core. On the contrary, if the sinter is too short, some of the liquid flowing along the wall may by-pass the sinter. For this reason, effects of sinter length on the liquid film flow rates have been investigated in the present report.

B. Pressure Drop

Since pressure drop is closely related to the liquid film flow rate, experimental data on pressure drop across the test section were taken. For this reason, a brief review of the literature available on this subject is given here.

The total static pressure drop along a test section may be split into three components--frictional loss, momentum change and elevation pressure drop arising from the effect of the gravitational force field. Thus the total static pressure drop may be written as

$$\left(\frac{\Delta P}{\Delta L}\right)_s = \left(\frac{\Delta P}{\Delta L}\right)_f + \left(\frac{\Delta P}{\Delta L}\right)_m + \left(\frac{\Delta P}{\Delta L}\right)_e \quad (2.1)$$

1. Frictional Pressure Gradient

A number of correlations are available for estimating the frictional pressure gradient for two-phase, adiabatic flow. Two principal correlations are the homogeneous model (16) and the slip model (20,21).

a. Homogeneous Model

This model presents a solution theoretical in nature which is not limited to any specific flow problem or substance. The basic assumptions on which the model is based are

(i) The flow is homogeneous and the linear velocities of gas and liquid are the same.

(ii) Thermodynamic equilibrium is attained between the two phases.

(iii) A suitably defined single-phase friction factor can be applied to the two phase flow to estimate the pressure gradient.

Owens (16) has derived equations for the calculation of pressure drop based on the homogeneous model. Frictional pressure gradient is given by the equation

$$\left(\frac{dP}{dL}\right)_f = \frac{2 f_{TP} G^2 \bar{v}}{D g_c} \quad (2.2)$$

The expression for two phase specific volume, \bar{v} , for homogeneous flow is written from the equation of continuity:

$$\bar{v} = \frac{\bar{V} A}{W_T} = \frac{W_g v_g + W_l v_l}{W_T}$$

$$\bar{v} = v_l + x (v_g - v_l) \quad (2.3)$$

All the terms in equation (2.2) above are definable except one, the two phase friction factor.

Owens (16) has suggested that the friction factor for the single phase liquid flow can be used for the two phase friction factor. McAdams, Woods and Heroman (17) have suggested the use of a weighted viscosity in the evaluation of Reynolds number for determination of two-phase friction factor. The mean viscosity is usually determined by the relationship

$$\frac{1}{\bar{\mu}} = \frac{1-x}{\mu_l} + \frac{x}{\mu_g} \quad (2.4)$$

Owens also points out that one should not expect his model to be valid for flow patterns in which the phases are completely separated such as occur with stratified and wave flow in horizontal channels.

The homogeneous model based on the definition of mean viscosity as given by equation (2.4) yields more accurate predictions in the high mass velocity ranges (18). Because of the assumption of equal velocities for both phases, one would expect this model to be more accurate for a fog or spray flow pattern occurring at high void fractions.

b. Slip Model

The slip model which has achieved the widest acceptance and is believed to have the best overall accuracy (18, 19) is that of Lockhart, Martinelli and Nelson (20, 21). This model is semi-empirical in approach and derives a value of pressure drop from a knowledge of overall liquid and gas flow rates, physical properties and channel dimensions alone, independent of the flow patterns.

The Lockhart and Martinelli model was successively developed in the period 1944-49 (20, 22, 23) from a series of tests on isothermal, two-phase, two-component flow in horizontal tubes at atmospheric pressure. These investigations were thus confined to the frictional component, $\left(\frac{\Delta P}{\Delta L}\right)_f$, of the equation (2.1). Four flow types were defined, depending on whether the flow would be turbulent or laminar when each phase was considered as flowing alone in the pipe. These flow mechanisms were:

(i) Flow of both the liquid and the gas may be turbulent. (turbulent-turbulent flow).

(ii) Flow of the liquid may be viscous and flow of gas may be turbulent (viscous-turbulent flow).

(iii) Flow of the liquid may be turbulent and flow of the gas may be viscous (turbulent-viscous flow).

(iv) Flow of both the liquid and the gas may be viscous (viscous-viscous flow).

Turbulent flow is said to exist for each phase if the Reynolds number for this phase flowing alone in the tube is greater than 2000. If the Reynolds number is less than 1000, laminar flow is said to exist.

The basic postulates upon which this analysis of pressure drop is based are

(i) Static pressure drop for the liquid phase must equal the static pressure drop for the gas phase regardless of the flow pattern as long as an appreciable radial static pressure difference does not exist.

(ii) The volume occupied by the liquid plus the volume occupied by the gas at any instant must equal the total volume of the pipe.

Three parameters relating the two phase to single phase pressure drops, were defined by Lockhart and Martinelli (20) as follows

$$\phi_g^2 = \frac{(dP/dL)_{TP}}{(dP/dL)_g}$$

$$\Phi_1^2 = \frac{(dP/dL)_{TP}}{(dP/dL)_1}$$

$$x^2 = \frac{(dP/dL)_1}{(dP/dL)_g}$$

Graphical relationships based on the collected experimental data were presented for the evaluation of either Φ_g or Φ_1 as a function of X for each type of flow.

It was soon recognised that all the data used to establish Φ_g or Φ_1 were essentially appropriate for only atmospheric conditions and that a pressure correction should be introduced for accurate predictions at all pressures. The Lockhart and Martinelli correlation was modified therefore by Martinelli and Nelson (21) to predict pressure gradients during forced circulation boiling of water. In this correlation, Martinelli and Nelson reported the ratio of local two-phase pressure gradient to the pressure gradient for 100% liquid flow as a function of quality and pressure in graphical form.

It was later found out that the two-phase pressure gradient depends, in addition to quality and pressure, on the total mass velocity (24, 25, 26). A correction factor for the effect of mass velocity on the pressure gradient has been derived by Jones (27).

2. Elevation Pressure Gradient

The elevation pressure gradient is evaluated by the relation:

$$\begin{aligned} \left(\frac{dP}{dL}\right)_e &= \frac{1}{\bar{v}} \frac{g}{g_c} \\ &= \frac{\bar{\rho}g}{g_c} \end{aligned} \quad (2.5)$$

where \bar{v} = Average specific volume of the mixture

For homogeneous flow, the expression for two-phase specific volume \bar{v} is given by equation (2.3).

For the slip model, the elevation pressure drop can be calculated using the value of the liquid hold-up, R_1 (defined as fraction of pipe volume filled by liquid). Thus

$$\left(\frac{dP}{dL}\right)_e = R_1 \rho_l + (1-R_1) \rho_g \quad (2.6)$$

Martinelli-Nelson correlation curves (21) gave R_1 as a function of quality and pressure. Sher (25) had found a slight inconsistency at low qualities in the Martinelli-Nelson curves. Applying Sher's correction, the Martinelli curves gave better agreement over the whole range of steam quality (19). The values of R_1 quoted by Sher for the modified Martinelli correlation are represented in the range 14.7 psia to 1000 psia by the empirical equation (19)

$$\frac{R_1}{1-R_1} = 9.77 \times 10^{-4} \left[(P + 85) \left(\frac{1-x}{x} \right) \right]^{0.7} \quad (2.7)$$

where P = system pressure, psia

x = the steam quality

3. Accelerational Pressure Drop

The pressure drop due to momentum change in the adiabatic system arises from the gas expansion due to the pressure gradient in the test section.

Two extreme cases can occur: One in which liquid and vapour are intimately mixed (fog flow) and the second in which liquid and vapour are completely separated.

In the second case, the liquid is not accelerated with the gas and hence the accelerational pressure drop can be much lower. However, when the liquid hold-up is high, the restriction of the gas to a smaller area of flow can reduce this difference (28).

The equations for calculating accelerational pressure drop are available for both conditions (16, 21). For annular flow, the real picture may be intermediate between the two since part of the liquid is intimately mixed with the gas phase in the form of small droplets and part flows separately in the form of a film on the tube wall.

However, at high pressures, the momentum pressure drop is only 1% or less of the total static pressure drop (24). This term has, therefore, been neglected in equation (2.1).

In order to estimate pressure gradient in the present report, both the homogeneous and the slip model were used. Equations (2.2) and (2.5) were used for the homogeneous-model calculations. For the ratio of local two-phase

pressure gradient to pressure gradient for 100% liquid flow given by the Martinelli-Nelson model, Jones' (27) polynomial fit was used. To facilitate calculations a computer program was written for this ratio as well as the mass - velocity correction factor.

The physical conditions used in predicting total pressure gradients were those at the mid-point of the test section. The quality in the test section was calculated from an energy balance.

C. Equilibrium Flow Pattern

In order that various theoretical analyses available for predicting liquid film flow rates may be applied to the experimental data, a fully developed flow pattern is desirable at the sinter. The flow is fully developed when the velocity and phase distributions do not change in the flow direction. Fully developed conditions are found only in the downstream sections of the channel where the inlet or entrance effects are negligible. Another requirement for fully developed adiabatic flow is that the pressure change in the flow direction be small enough for the liquid and gas properties to remain relatively constant.

The mode of introduction of water and steam, into the test section affects considerably the length for the flow pattern to develop fully (29,30,14). If the water is injected smoothly through porous walls, there is no immediate entrainment and it takes considerable time and length to establish the flow pattern. However, if the suspended

droplets of water are already present in steam, they are redeposited on the wall, thus eventually setting up an equilibrium condition. The time and length required in the second case are much less than that in the first. Therefore, it is desirable to introduce water in the mixer in the form of a spray. The liquid should be sliced off the tube wall of the mixer before introducing it into the test section so that equilibrium is attained in a shorter length.

One way to test whether equilibrium conditions have been achieved in the test section is to find the liquid film flow rates at various lengths along the test section (15). Conflicting observations have been reported as to the length of the test section in which the equilibrium flow pattern is achieved (8,31.32). The assumption that equilibrium flow pattern would be achieved in a length of about 200 diameters may not be too far from reality. In this equilibrium situation, the rate of deposition of droplets onto the film will be equal and opposite to the rate of entrainment of droplets from the waves to the core.

However, it must be mentioned that the pressure gradient along the channel results in a gradual increase of steam velocity which, in itself, leads to gradually increasing entrainment. Therefore, an assumption of complete equilibrium is not valid.

D. Models for Predicting Liquid Film Flow Rates

Many theoretical models for two-phase annular flow have been proposed. Reviews of papers up to 1958 have been made by Charvonia (33) and Bennett (34). The theories of Anderson and Mantzouranis (35) and Calvert and Williams (36) applied the classical work of Von Karman, Prandtl and Nikuradse for single-phase flow to evaluate the velocity profile in the liquid film for two-phase annular flow. Film flow rates were then obtained by integrating these velocity profiles. In Dukler's analysis (37) for downwards annular flow, the velocity profile of the film on the wall was assumed to be given by Deissler's and Von Karman's relations. This analysis was improved and modified for the case of upwards flow by Hewitt (38). All the preceding models considered only the simplified case of a liquid film and gas core with a smooth interface and no liquid entrainment.

In a recent paper, Levy (1) has presented a semi-empirical model for the prediction of liquid film flow rates in annular flow with entrainment. He considered the momentum and mass-transfer component of the interfacial shear. Levy showed that the momentum term is dominant within the liquid film while the mass-transfer term is the important component within the gas core.

Assuming that the liquid film thickness is small and that the gas density is much smaller than the liquid density,

Levy arrived at the following simplified equation:

$$\sqrt{\frac{(-dp/dL)(D/4) \rho_c}{\rho_l}} \frac{\rho_g}{G_g} R\left(\frac{\rho_l}{\rho_g}\right) \left(\frac{\rho_l}{-dp/dL}\right)^{-n} = F\left(\frac{2t}{D}\right)$$

where t = thickness of the film

G_g = gas phase mass flux

$n = 0$ if $(dp/dL) \geq \frac{g}{g_c} \rho_l$

$= 1/3$ if $(dp/dL) < \frac{g}{g_c} \rho_l$

In the above equation, the function $R(\rho_l/\rho_g)$ was introduced from semi-empirical considerations to account for slip of the gas with respect to the liquid particles contained in the core. Universal application of the function $F(2t/D)$ was established by using data taken by the CISE (39) team at various liquid and gas phase densities and over a wide range of liquid and gas flow rates.

By analogy with single phase flow, velocity profiles in the liquid film were evaluated. Film flow rates were obtained by integrating these velocity profiles. The treatment was limited to situations where y^+ , the Reynolds number based on the friction velocity, was greater than 30.

The correlation obtained was tested with film flow rate data for air-water mixtures obtained by Gill and Hewitt (14) at near atmospheric pressure. As pointed out by Levy, the proposed model gave an approximate, yet acceptable, prediction of film flows for two-phase annular flow. One set of calculations was performed for upwards flow of

steam-water mixture at a pressure of 1000 psia in a smooth 1/2-inch diameter pipe. However, no experimental data were available then to confirm these calculations. Need for taking additional experimental data was pointed out by Levy to further check and improve the analytical model.

A second analytical model for predicting entrainment in adiabatic, annular flow conditions was given by Minh and Huyghe (2). It was postulated that the entrainment fraction is a function of the volumetric kinetic energy of the core of the flow considered as a homogeneous mixture of gas and liquid droplets in suspension. Semi-empirical correlations were presented relating entrainment fraction to the kinetic energy of the core of the flow for water-air and alcohol-air mixture. An attempt has been made in the present work to check if the same correlation holds for steam-water mixtures.

III. THEORY

A. Slug-Annular Flow Transition

Since the purpose of the study was to measure the liquid film flow rates, then all data must be taken in a mass velocity--quality range where the flow is annular. In annular flow, the liquid travels up the side of the tube with a velocity less than that of the gas which travels up the core. Part of the liquid is entrained in the gas core as droplets and as the gas velocity increases, the entrainment also increases.

Several investigators have reported the experimental conditions for the existence of different types of flow patterns. However, little work has been done with steam--water mixtures at high pressures. The general practice has been to apply flow pattern results obtained at low pressure to the required conditions at high pressures. As pointed out by Baker (40), the use of the results from the low pressure studies for the application to high-pressure situations requires that the correct similarity parameters be known or that the correct governing equations for the phenomena under consideration are obtainable. This question has not been resolved yet.

One of the notable works in the field of slug-annular flow transition is that of Griffith (41). Griffith reported that the slug-annular flow regime transition occurs at almost constant quality at a particular pressure and this transition is independent of the flow rate as long as

$$\frac{V_{gs}^2}{g D} \frac{\rho_g}{\rho_l} \geq 2$$

where V_{gs} : superficial vapour velocity

D : Pipe Diameter

ρ_g : Vapour density

ρ_l : Liquid density

The transition quality varied from 8.6% at 215 psia to 17.6% at 615 psia and by extrapolation, transition quality at any other pressure can be determined. However, Griffith used a contact probe to detect the slug--annular transition in which case erroneous readings could be obtained even when the flow is clearly annular. This is due to the large disturbance waves which throw out "streamers" of liquid and break up into droplets (42).

Another outstanding contribution is that of the Harwell group (42). Investigation of flow patterns in a 0.497 in I. D. tube for steam-water flow generated by boiling at pressures of 500 and 1000 psia was carried out by this group. Different flow patterns were observed using high speed cine photography of the flow emerging from the end of the heated

section into a glass tube of equal diameter. This group concluded that the transition to annular flow does depend on the exit quality in addition to the total mass flux. Two flow pattern diagrams at pressures of 500 and 1000 psia were presented.

At present it is not known if the transition does occur at a constant quality as observations by different workers are conflicting. As pointed out by Kirby (8), the results of visual observations made at the exit of a heated round tube using Freon-12 at 155 psia (which simulates water at 1000 psia) showed that the quality at the onset of climbing film flow could vary from 5% to 25% depending on the heat flux, mass flow rate and inlet sub-cooling. Observations by Tippets (43) agree fairly well with those of Griffith as do the visual observations of Hostler (8, 44).

Wallis (45) suggests that the transition to annular flow in a vertical tube at low liquid velocities is not influenced by the liquid flow rate so long as liquid velocity is not very high. The minimum gas velocity at which this transition occurs is given by the equation:

$$V_g = V_g^* \rho_g^{-\frac{1}{2}} \left[D_g (\rho_l - \rho_g) \right]^{\frac{1}{2}}$$

where: V_g : Gas velocity

D : Tube diameter

ρ_l : Liquid phase density

ρ_g : Gas phase density

V_g^* is a dimensionless parameter and a value of 0.8-0.9 for V_g^* was given by Wallis as representing the transition to annular flow. However, recent work (42, 46) has shown that a value of unity for V_g^* more correctly represents this transition.

By making use of the above relation, the transition to annular flow is found to occur at a minimum steam velocity of 5.1 feet/sec at 1000 psia. The mass flow rate corresponding to this velocity is about 50 lbm/hour. For the present report, different water flow rates were selected at this or higher values of steam flow and the total mass flux calculated. A flow pattern diagram at 1000 psia in reference (42) was then used to determine if the flow regime was annular.

B. Liquid Film Flow Rate

While attempting to remove the liquid film completely through the sinter, small amounts of the steam phase will inevitably be removed from the core. The two-phase mixture thus extracted is passed through a cooler and is condensed. In order to estimate the amount of liquid extracted, use is made of the following equation, obtained by carrying out a heat balance over the cooler:

$$W_w = \frac{W_e H_s - W_e (T_7 - 32) C_p - W_c (T_9 - T_8) C_p}{H_s - H_w} \quad (3.1)$$

where W_e : mass flow rate of extract

- W_w : mass flow rate of liquid
 H_s : enthalpy of steam at the sinter
 H_w : enthalpy of water at the sinter
 W_c : coolant flow rate
 T_7 : temperature of extract at outlet of the cooler
 T_8 : inlet temperature of coolant
 T_9 : outlet temperature of coolant

The derivation of this equation is given in Appendix I. All properties should be based on the temperature and pressure on the inside of the sinter. This is because some of the water film, while passing through the sinter, flashes into steam due to a pressure differential across the sinter.

A record is made of the total flow through the sinter and of the pressure differential across it. The flow rate is changed by varying the pressure differential across the sinter. By use of equation (3.1) above, liquid flow rates through the sinter are calculated.

Staniforth (4) suggested that pressure differentials across the sinter should be plotted against flow rate as shown in Figure 1. The liquid film flow rate rises to a constant value and remains there despite further increase in the pressure differential. Any increase in pressure differential will only increase the amount of vapour drawn through the sinter. The appearance of the plateau in these experiments was interpreted, therefore, as indicating that all the liquid film flowing along the wall had been extracted.

However, one would expect to obtain this type of curve only in cases where the exit quality is very high. At lower qualities, liquid from the core will be removed continuously after the liquid flowing along the tube wall has been extracted. Since a wide range of exit qualities was used by Staniforth (4), the existence of a plateau did not always suffice to determine the film flow rates. In cases where the plateau was not clearly distinguishable, the film flow rate was determined by judging the position on the curve beyond which the vapour flow rate increases rapidly with increasing pressure differential. Figure 2 from reference(4) shows an example of the choice of this position.

This method of finding the liquid film flow rate was not found to be convenient or accurate, especially at low qualities. It was not possible to judge accurately the position on the curve beyond which the vapour flow rate increases rapidly with increasing pressure differential. In the present report, therefore, steam flow rate through the sinter was plotted against water flow rate as shown in Figure 3. Two distinct portions of the plot, both straight lines, are noticed. The point at which the steam flow rate increases rapidly is given by the intersection of these two lines which, in turn, gives the liquid film flow rate. This method of finding the liquid film flow rates was found to be easy, reproducible and is probably more accurate than the one given by Staniforth (4).

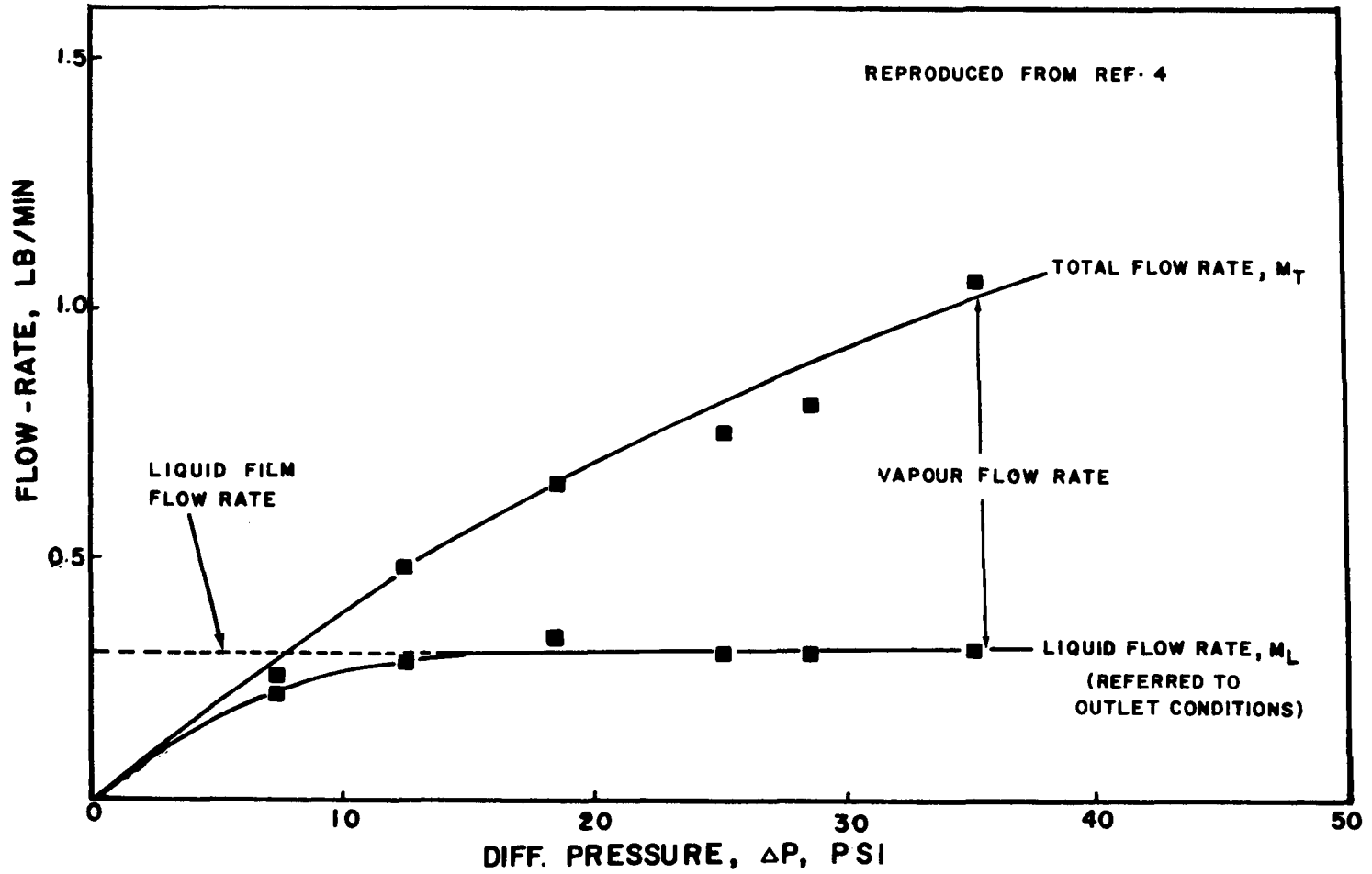


FIG. 1 TYPICAL PLOT OF FLOW-RATE & DIFFERENTIAL PRESSURE FOR HIGH EXIT QUALITY.

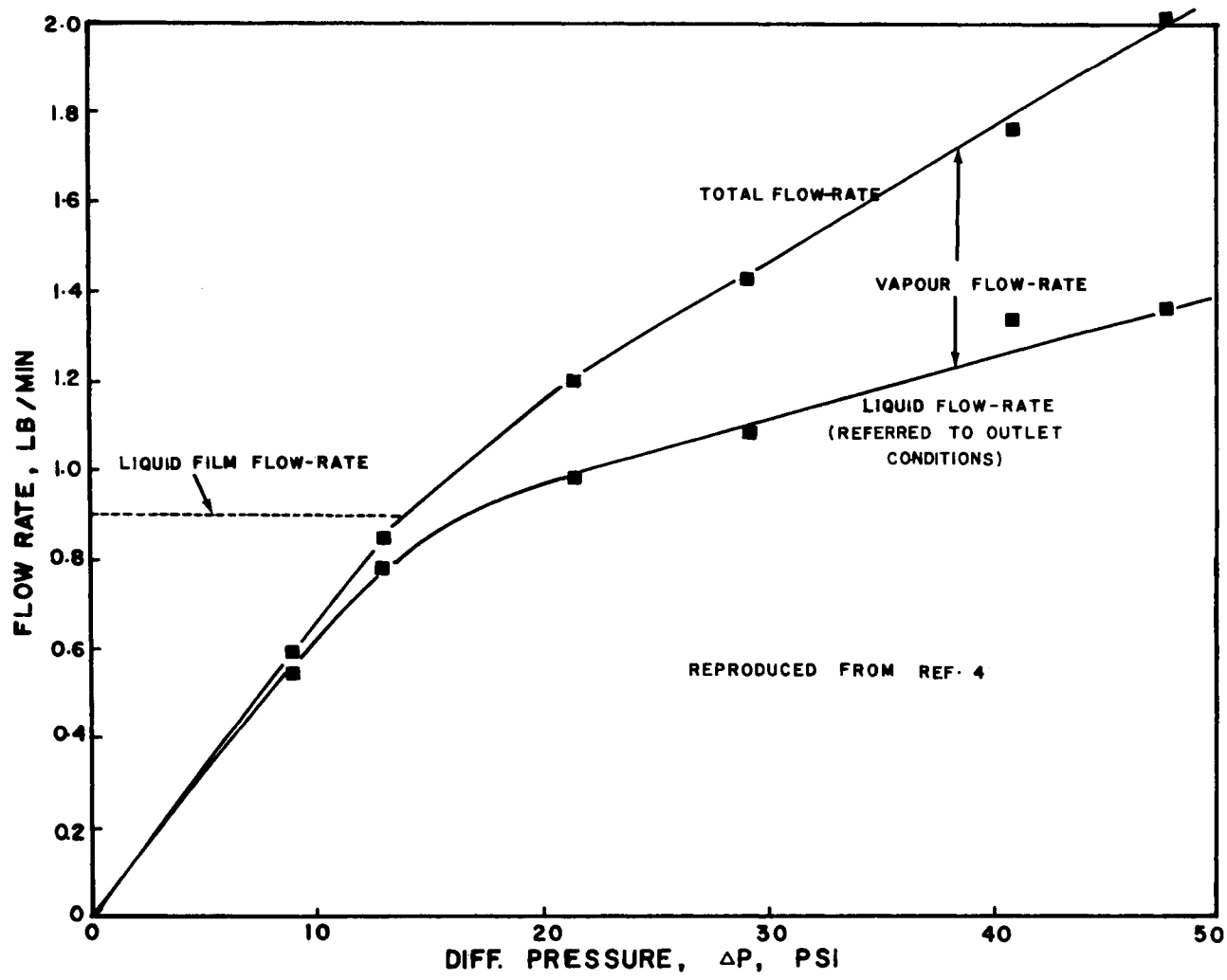


FIG.2 TYPICAL PLOT OF FLOW RATE & DIFFERENTIAL PRESSURE FOR LOW EXIT QUALITY

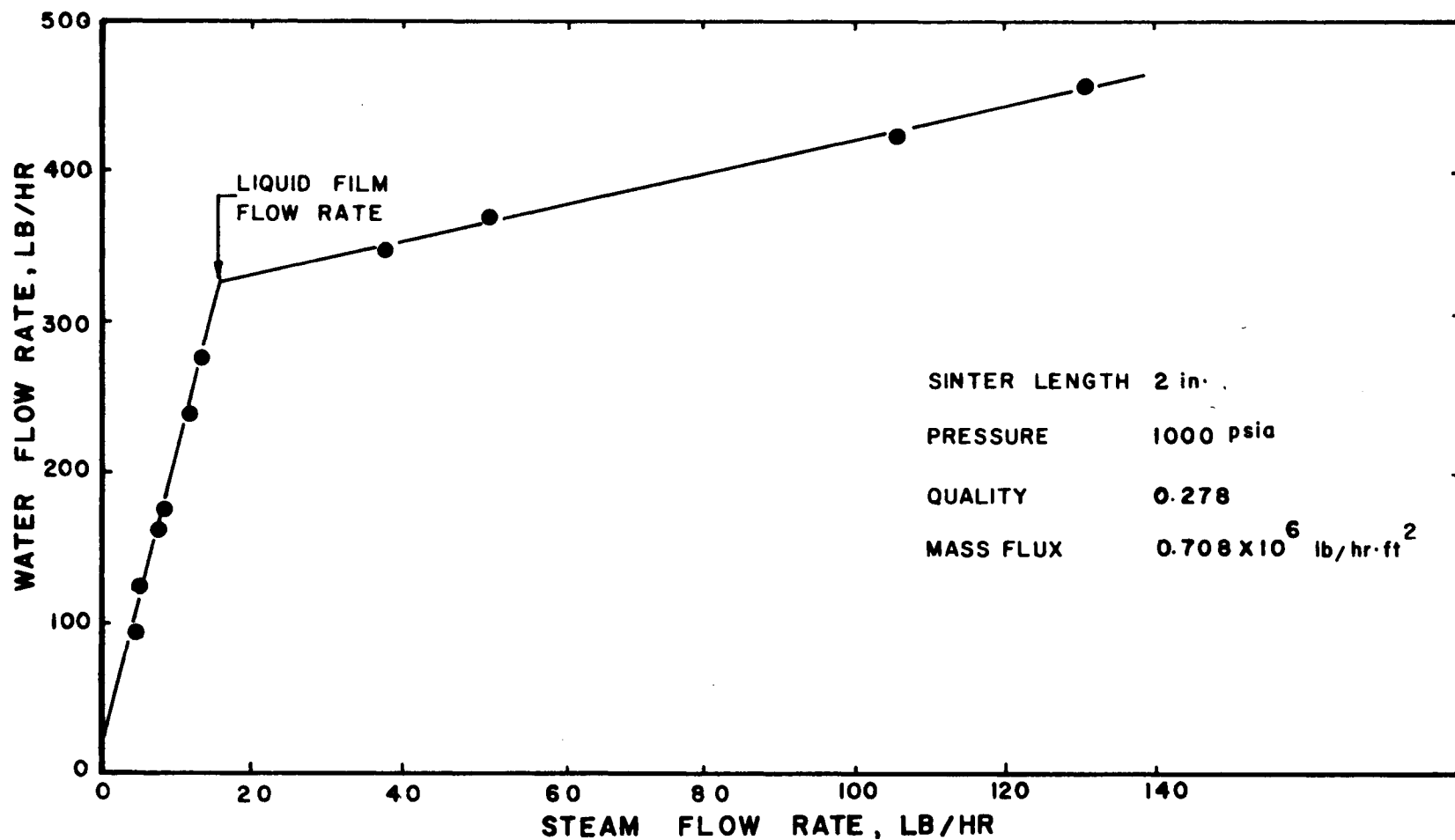


FIG. 3 TYPICAL PLOT OF STEAM FLOW-RATE & WATER FLOW-RATE THROUGH THE SINTER.

IV. EXPERIMENTAL EQUIPMENT AND PROCEDURE

A. Equipment

The experimental equipment consisted essentially of a test section, two high pressure boilers, a preheater, a superheater, a condenser, two high pressure pumps, two coolers, a mixer and a number of flow measuring devices.

A schematic diagram of the high pressure experimental loop is given in Figure 4. Steam from the electrically heated boilers passed through a superheater, an orifice plate connected to a D. P. cell and then via a throttle valve to the mixer. The superheater was electrically heated and consisted of three hairpin elements having a power rating of approximately 7 kw each.

A Bingham high pressure centrifugal pump of capacity 36 IGPM at 300 feet head supplied water to the preheater. An orifice plate and a throttling valve measured and metered the flow to the mixer. In the preheater were three heating coils with a power rating of 12 kw each and one heating coil with a power rating of 72 kw.

Steam-water mixtures from the mixer passed up the vertical test section. The high pressure test section was made from a 3/8-in stainless steel (type 304), Sch 40 pipe, with an inside diameter of 0.493 in (thickness 0.091 in). Test

section details and the position of various pressure taps are detailed in Figure 5. Three pressure taps were provided along the length of the test section at intervals of 3.5 feet. Each pressure tap consisted of four 1/16 inch diameter equispaced holes around the pipe perimeter. One pressure tap was at a distance of about 6 inches upstream from the sinter. Due to the design of the sinter chamber, it was not possible to locate a pressure tap any closer to the sinter. The sinter chamber was designed to accommodate sinters of various lengths.

The stainless steel sinter was mounted approximately 7-1/2 feet from the inlet of the test section. By means of this sinter, it was planned to extract the liquid film flowing on the pipe wall. The liquid, together with small amounts of steam from the main core, passed through a cooler C₁ (Figure 4) which consisted of a 3/16 inch O.D. coiled pipe in an annular bath of cooling water.

The steam-water mixture from the top of the test section passed to a water cooled condenser. From the condenser, water flowed to the inlet of the main centrifugal pump. Because of the high capacity of the pump, a large portion of the water was recirculated through a by-pass valve. Another portion was taken to the cooler C₂ (Figure 4) where it was cooled for use in the condenser.

Make-up water for the liquid extracted through the sinter was provided by a high-pressure Aldrich reciprocating

- C COOLER
- M MIXER
- MU MAKE-UP PUMP
- MP MAIN PUMP
- PPC PNEUMATIC PRESSURE CALIBRATOR
- R ROTAMETER
- SC SINTER CHAMBER
- SS SUPERHEATER
- OT OVERHEAD TANK
- T THERMOMETER
- T_c THERMOCOUPLE
- P PRESSURE TAPS
- CV COLLECTION VESSEL

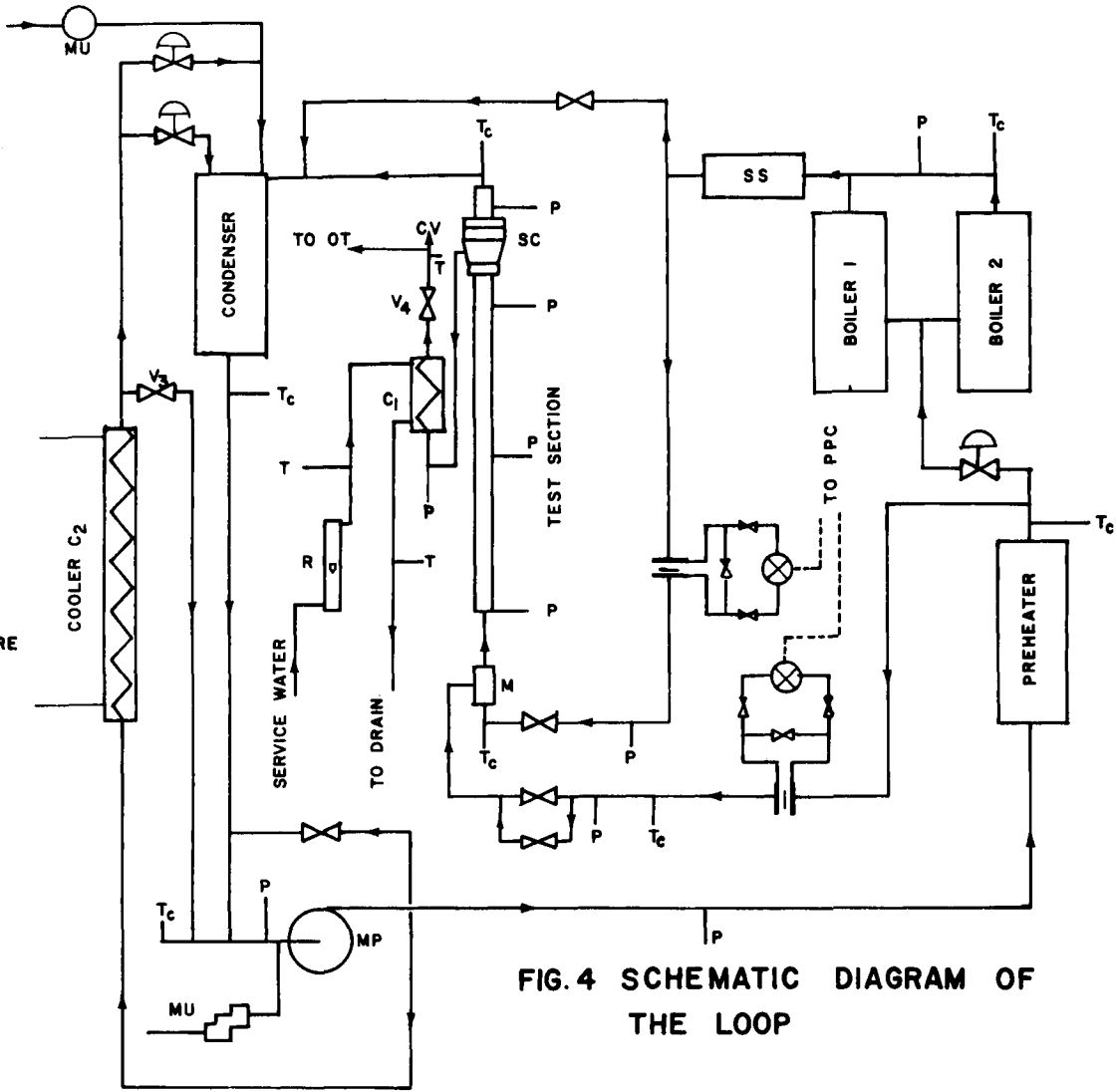


FIG. 4 SCHEMATIC DIAGRAM OF THE LOOP

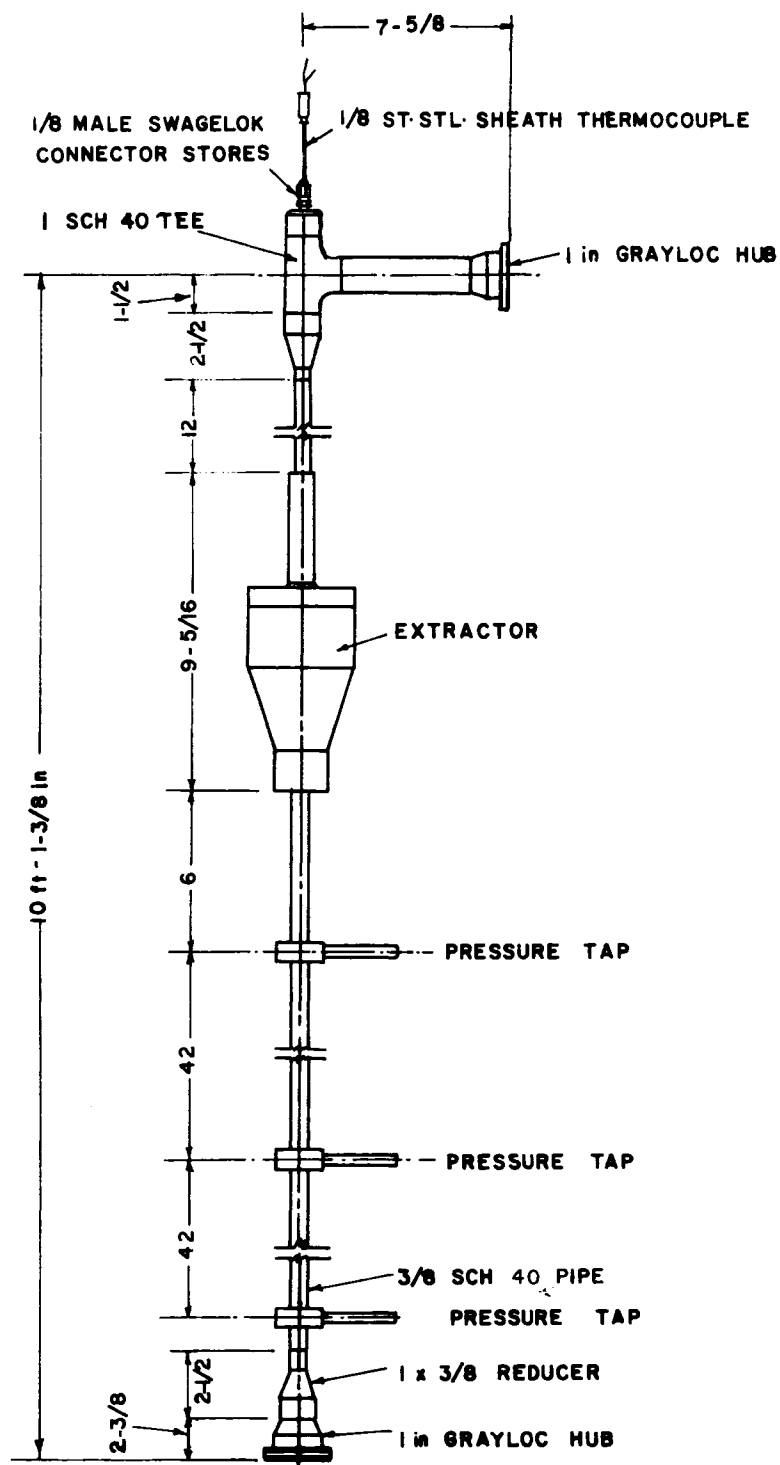


FIG. 5. TEST SECTION DETAILS
 ALL DIMENSIONS IN INCHES

pump. It was pumped from the overhead storage tank into the condenser. A second make-up pump of smaller capacity was also available which pumped water from the storage tank to the inlet of the main centrifugal pump. Pressure in the condenser was controlled automatically.

B. Measurement of Loop Variables

1. Pressure Measurement

Two types of pressure measurements were made: total pressure and pressure differentials across the test section and across the various orifice meters.

a. Total Pressure

The following pressure measurements were made with a Heise pressure gauge:

(i) Steam and water pressures at inlet to the mixer,

(ii) Pressures at inlet and exit of the test section.

The dial face of the gauge was graduated in 5 psi increments from 0 to 4000 psig. The gauge was calibrated by using a dead-weight tester and found to be accurate within the reading error.

b. Pressure Differential

Pressure differential measurements across the flow metering orifices were made with Foxboro, Type 13A, differential pressure cells calibrated in the appropriate range. The pressure signal from the D. P. cell was transmitted to a Wallace and Tiernan Precision Pneumatic Calibrator

which is accurate to one part in one thousand of full scale range. Each orifice meter was connected to two D. P. cells with ranges of 0-25 inches and 0-100 inches of water.

For the pressure differential across the test section, a D. P. cell with a range of -50 to +150 inches of water was employed. The Wallace and Tiernan gauge was used to measure the cell output.

2. Temperature Measurements

Six important temperature measurements were made: water and steam temperatures at the inlet to the mixer, temperature at the exit of the test section, inlet and outlet temperatures of the cooling water and outlet temperature of the condensate from the cooler.

The first three temperature measurements were made with Chromel-Alumel thermocouples (constructed by welding in an oxy-acetylene flame) encased in 1/8-inch stainless steel sheaths. All thermocouple wires led to the potentiometer through a junction box and a selector switch. The steam thermocouple was calibrated in place using saturated steam at various pressures in the test section. The saturation temperature corresponding to the known pressure was determined from steam-tables. The thermocouple was found to be accurate within -2°F and appropriate corrections were applied to all temperature readings. Thermocouple potentials were read to 0.01 mV which corresponds to about 0.45°F . A Joseph Kaye Model 1150 ice-point reference system was used with all

Chromel-Alumel thermocouples to provide a cold junction reference temperature accurate to $+0.05^{\circ}\text{C}$ from true 0°C .

Inlet and outlet temperatures of the cooling water and the outlet temperature of condensate from the condenser were measured by using Fisher thermometers with a range of -1 to 51°C and graduated in 0.1° increments. The accuracy expected with the thermometers was of the order of 0.05°C .

3. Flow Measurements

Various flow measurement techniques were utilized for determining the loop flow parameters. The choice in each case was dictated by the requirements of pressure, temperature and readout at operating conditions.

a. Test Section Input

Orifice meters with D. P. cells were used to measure the inlet water and steam stream flow rates. Flow rates were adjusted by throttling valves downstream of the orifice. The orifice plates were calibrated previously by direct weighing techniques using water at about 140°F . The discharge coefficients thus obtained were assumed to apply for steam at the corresponding Reynolds numbers. Orifice differentials corresponding to any required flow rates were obtained from a series of tables produced by use of a computer. The flow rates measured in this manner were estimated to be accurate to within $\pm 2\%$. Oscillations of the system and reliance on the D. P. cell coupled with the pneumatic calibrator might have increased the likely error

to the order of $\pm 4-5\%$.

In order to cover the whole flow range using only the two D. P. cells with ranges of 0-100 and 0-25 inches water, five orifices of different diameters were chosen as follows:

	Diameter inches	Flow range lb/hr
Steam orifices	0.2516	50-155
	0.495	150-625
	0.647	400-1200
Water orifices	0.124	50-235
	0.2508	200-850

b. Extract Coolant

Cooling water flow required to condense and cool the extracted flows from the test section was measured with a Brook's rotameter, type 12-1110-24, of range 1.6-28 GPM and scale length 600 mm. It was calibrated by the direct weighing technique as a check on the manufacturer's accuracy claims and was found to be accurate within $\pm 1\%$. Calibration data thus obtained were curve-fitted and used for the calculations.

c. Experimental Procedure

Before any data were taken, the loop was pressurized with water up to 1200 psig to check for any leaks in the system.

Experimental runs were taken by introducing two separate streams of steam and water through the mixer to the test section inlet. The flow rates of both streams were adjusted, by throttling valves downstream of the

orifices, as nearly as possible to the required conditions at the test section inlet. Power to the steam superheater was adjusted so that the steam at the mixer inlet was about 10°C superheated. The water stream flowed through a preheater which raised its temperature to a few degrees below saturation. The basis of determining steam superheat and the water sub-cooling was the accurate measurement of the pressure and obtaining the equivalent saturation temperature. Final adjustment to the flow rates was made when steady state conditions were achieved. To control the water temperature accurately within 2 or 3°C , it was necessary to adjust the inlet temperature of water to the preheater. This was accomplished by changing the flow rate of water to cooler C_2 by means of valve V_3 (Figure 4).

When steady state conditions were achieved, control valve V_4 (Figure 4) was opened to adjust the pressure differential across the sinter so as to get a small extraction rate. The coolant water flow was adjusted so that temperature difference between inlet and outlet was about 10°C . Thermocouple, thermometer, D. P. cell, rotameter and pressure readings were recorded. For each run total mass flux, quality, sinter length and pressure were kept constant but different extraction rates through the sinter were obtained by varying the pressure differential across it. One of the four independent variables (mass flux, quality, sinter length and pressure) was then varied and the previous set of data

taken for the new experimental conditions.

The range of experimental parameters is shown in Table 4.1.

TABLE 4.1
RANGE OF EXPERIMENTAL PARAMETERS

Parameter	Range
Quality	0.3 - 0.92
Total mass flux	$0.2 - 0.7 \times 10^6 \frac{\text{lbm}}{\text{hr.ft}^2}$
Pressure	1000, 1200 psia
Sinter length	2, 1, 1/2 in

V. RESULTS AND DISCUSSION

The effect of four independent variables on film flow rates was investigated in the present report: total mass flux, steam quality, pressure and sinter length. A large fraction of the data were taken at a pressure of 1000 psia with a few runs at 1200 psia. It was planned originally to investigate the effect of sinter grades on the liquid film extractions by employing at least three different grades of sinters. Due to a shortage of time, this phase of the study could not be carried out.

Experimental data were obtained over approximately 27 working days with eight hours of operating time per day. The number of runs taken with different sinter lengths is shown in Table 5.1.

TABLE 5.1
SUMMARY OF EXPERIMENTAL DATA

Sinter length in.	Pressure psia	Number of runs
2	1000	18
	1200	4
1	1000	13
1/2	1000	11
	1200	3

A complete compilation of all the results is given in Appendix II. In the early stages of this work, some of the pressure drop data could not be recorded since a pressure differential cell with the proper range was not available.

A. Pressure Drop

Pressure drops across the test section were calculated using models proposed by Martinelli and Nelson (21) and by Owen (16). Physical properties used in these analyses were based upon conditions at the middle (axially) of the test section.

Briefly, two routes were followed to calculate pressure drops using Owen's homogeneous model. In one of them, the two-phase friction factor, f_{TP} , is based on the single phase liquid flow ($f_{TP}=f_1$) as suggested originally by Owen. In the other, a two-phase friction factor, \bar{F} , was based on the mean viscosity, $\bar{\mu}$, as defined by equation (2.4). The results for both of these approaches are plotted in Figures 6 and 7. It is seen that agreement of predicted values of pressure gradient with the experimental values is slightly better with $f_{TP} = \bar{F}$.

Experimental pressure gradients have been plotted against predicted values from the Martinelli and Nelson model in Figure 8. It is observed that Jones' correction factor for the mass-velocity effect over-corrects the pressure gradient as predicted by the model.

Owen's model gives much better agreement with the

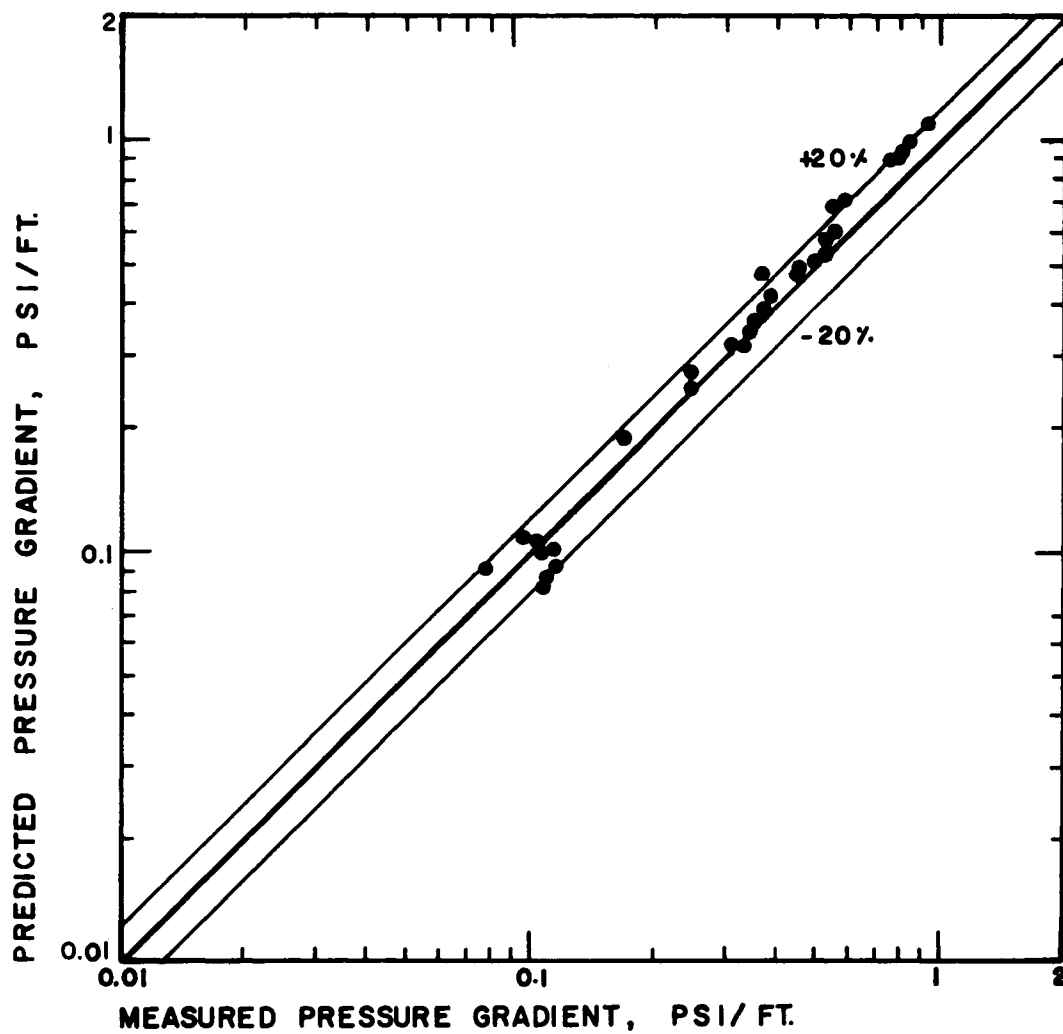


FIG.6 COMPARISON OF OWEN'S MODEL WITH
EXPERIMENTAL DATA ($f_{tp} = f_i$)

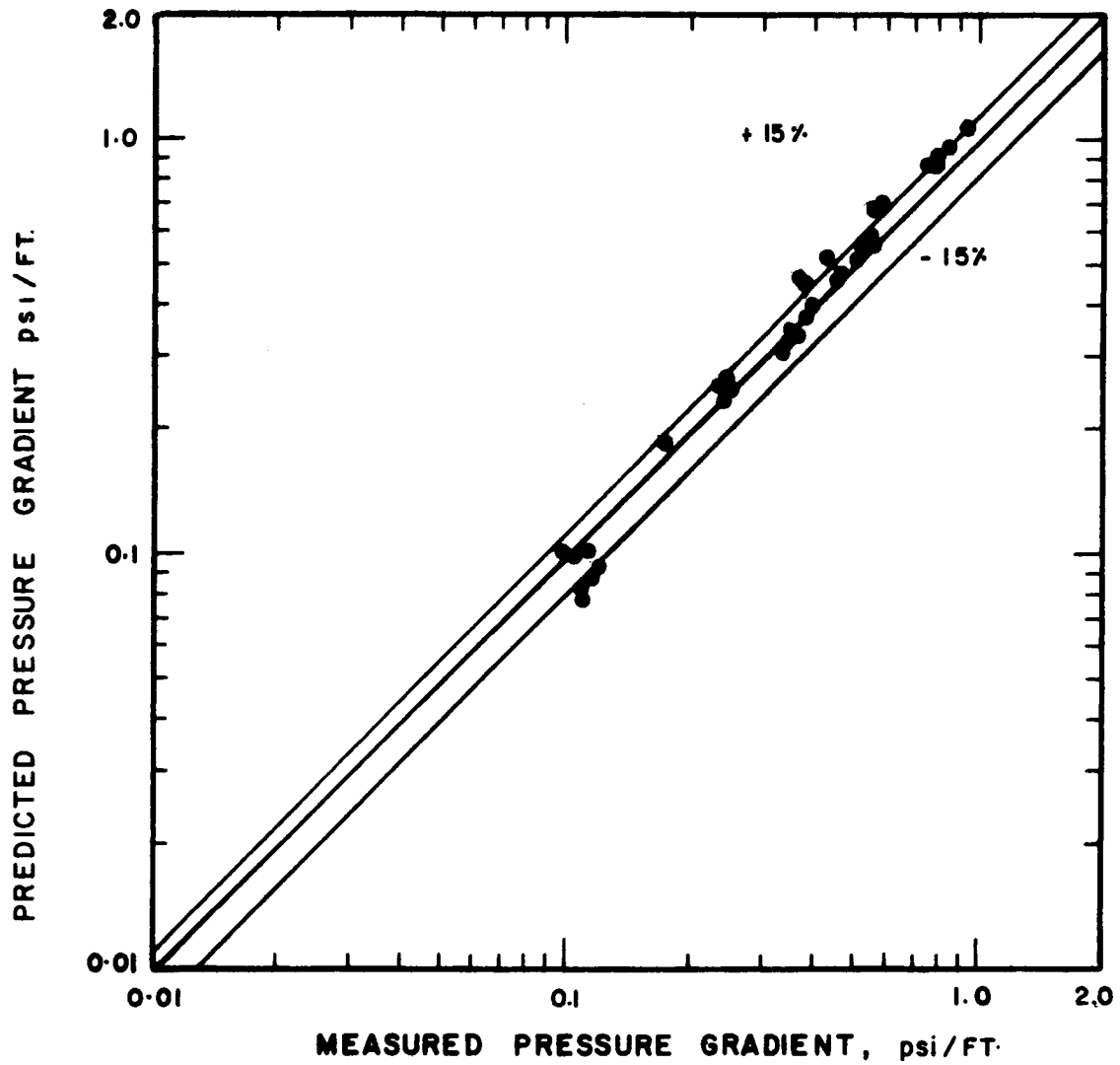


FIG. 7. COMPARISON OF OWEN'S MODEL WITH EXPERIMENTAL DATA ($f_{tp} = \bar{f}$)

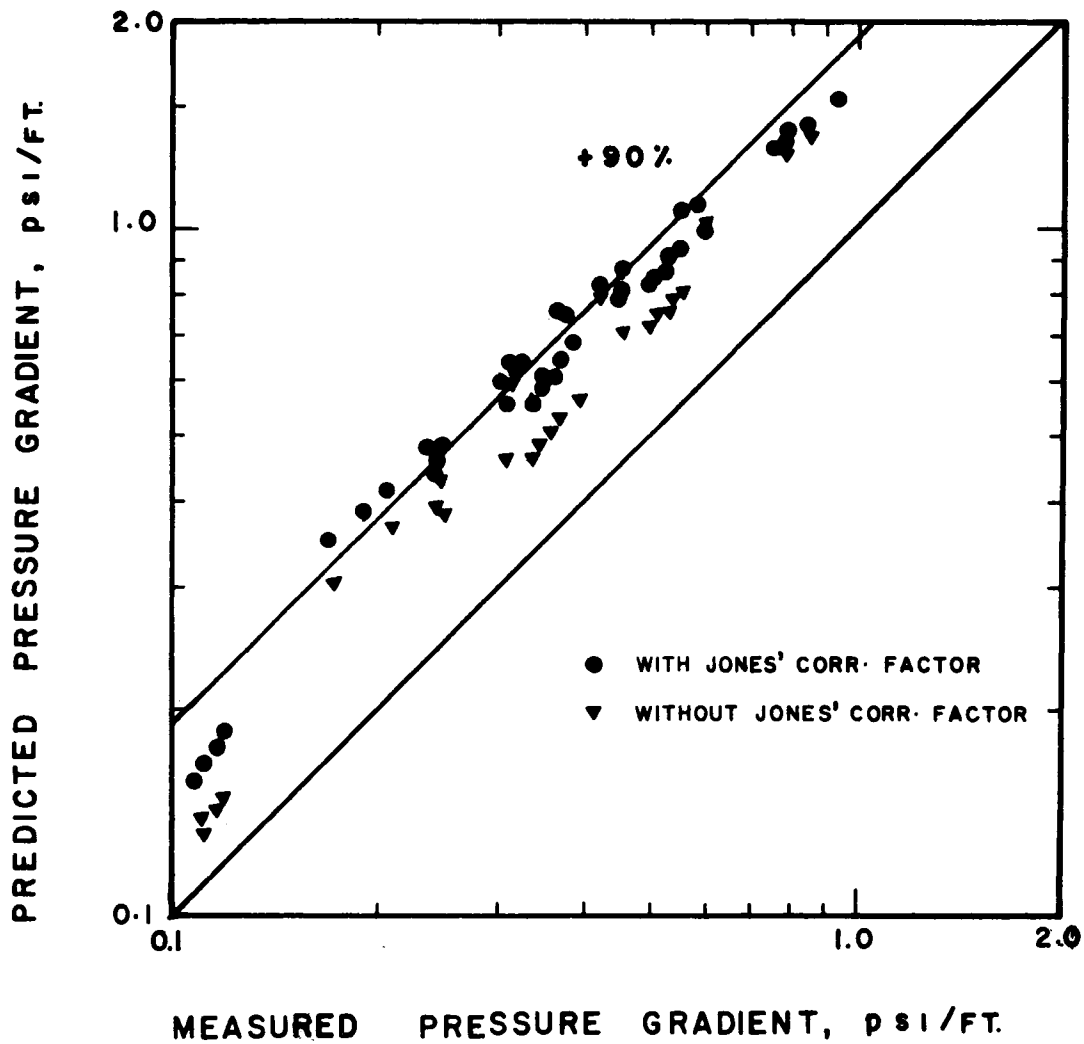


FIG. 8. COMPARISON OF MARTINELLI & NELSON MODEL WITH EXPERIMENTAL DATA.

experimental data as compared to Martinelli and Nelson predictions. This is probably due to the fact that the basic assumption of equal velocities for gas and liquid phases, on which Owen's model is based, is approached more closely in annular flow.

B. Liquid Film Flow Rates

The variation of experimental liquid film flow rates with quality at constant total mass flux and pressure has been shown in Figures 9 to 11 for three different sinter lengths. Liquid film flow rates have been plotted as a function of total mass flux at constant quality in Figure 12. The liquid film flow rate decreased with increased steam quality and total mass flux. Qualitatively, this behaviour is physically consistent and confirms the trends predicted by Levy's analysis (1) of two-phase annular flow.

However, a careful study of the experimental results showed that the liquid film flow rates, at a steam quality of approximately 0.3 and total mass flux of 0.5×10^6 lbm/hr.ft², were less than the corresponding film flows at the same quality but higher total mass flux (0.7×10^6 lbm/hr.ft²). This same trend is shown by runs 24 - 26 taken at a total mass flux of approximately 0.2×10^6 lbm/hr.ft² and steam quality of 0.8. This behaviour is not consistent with the general trend of the data. The discrepancy can probably be explained by reference to the flow pattern diagram for steam/water flow at 1000 psia (Fig. 13) reproduced from reference (42). At a total mass flux of 0.2×10^6 lbm/hr.ft²,

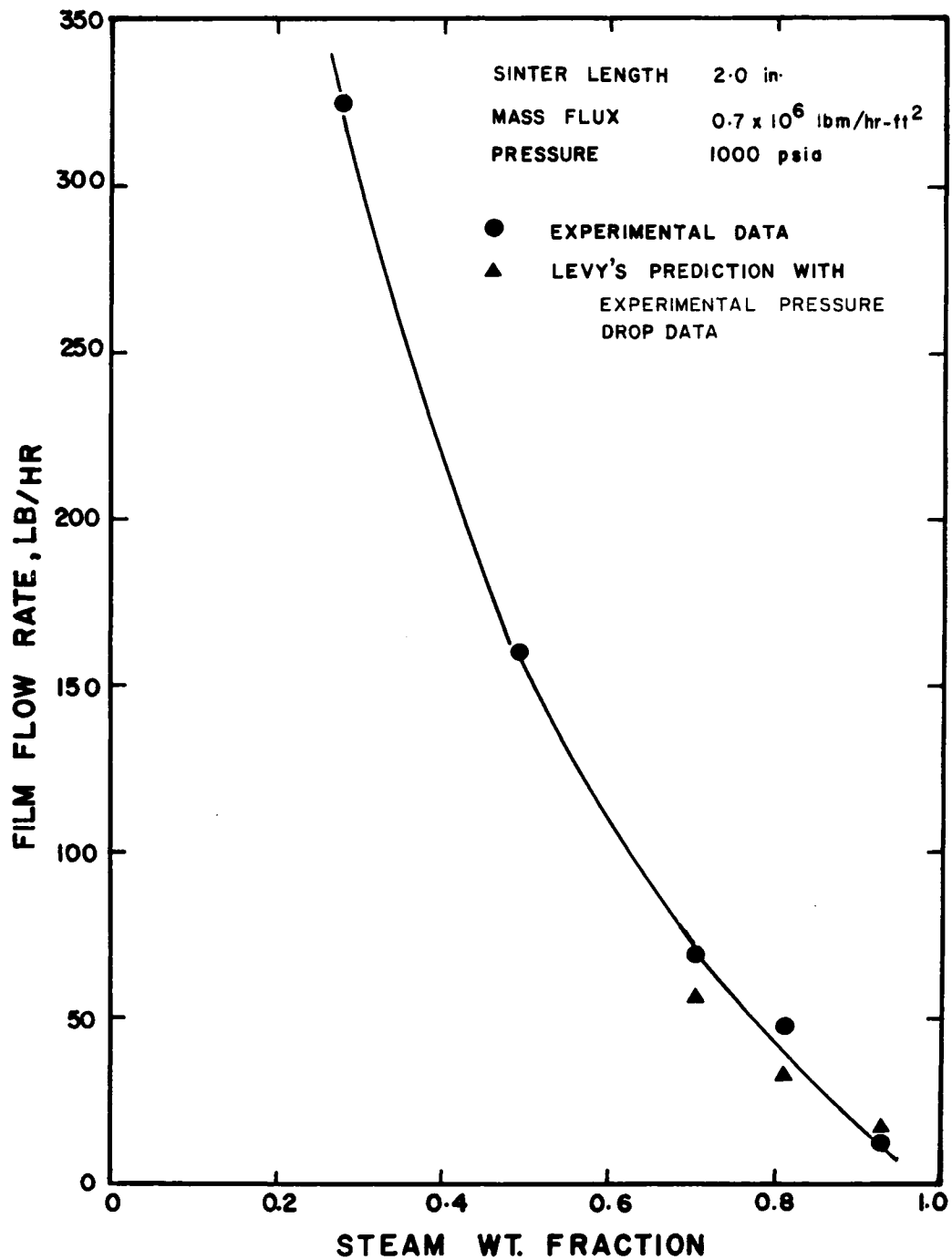


FIG.9 VARIATION OF FILM FLOW RATES WITH QUALITY

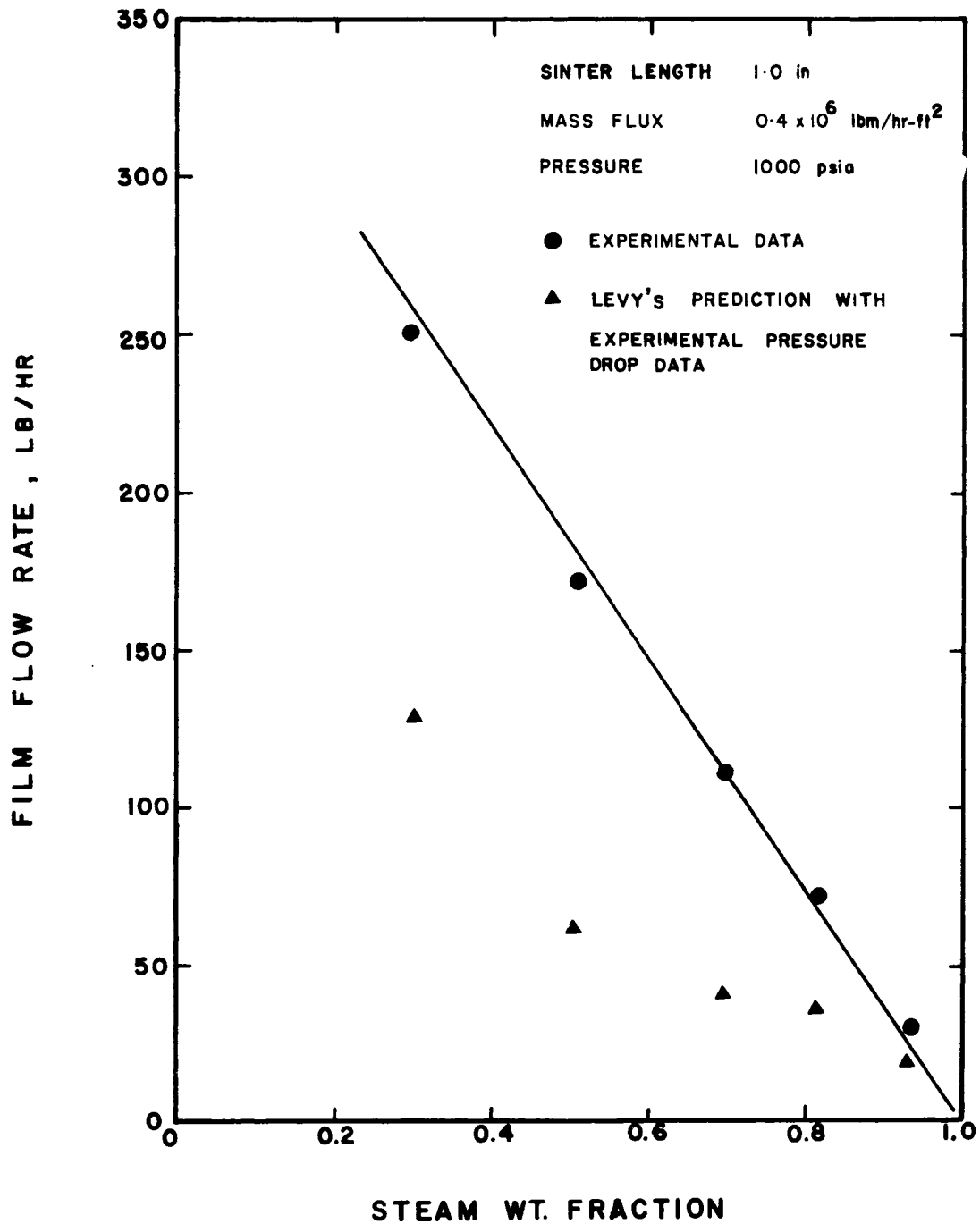


FIG.10. VARIATION OF FILM FLOW RATES WITH QUALITY

UNIVERSITY OF WINDSOR LIBRARY

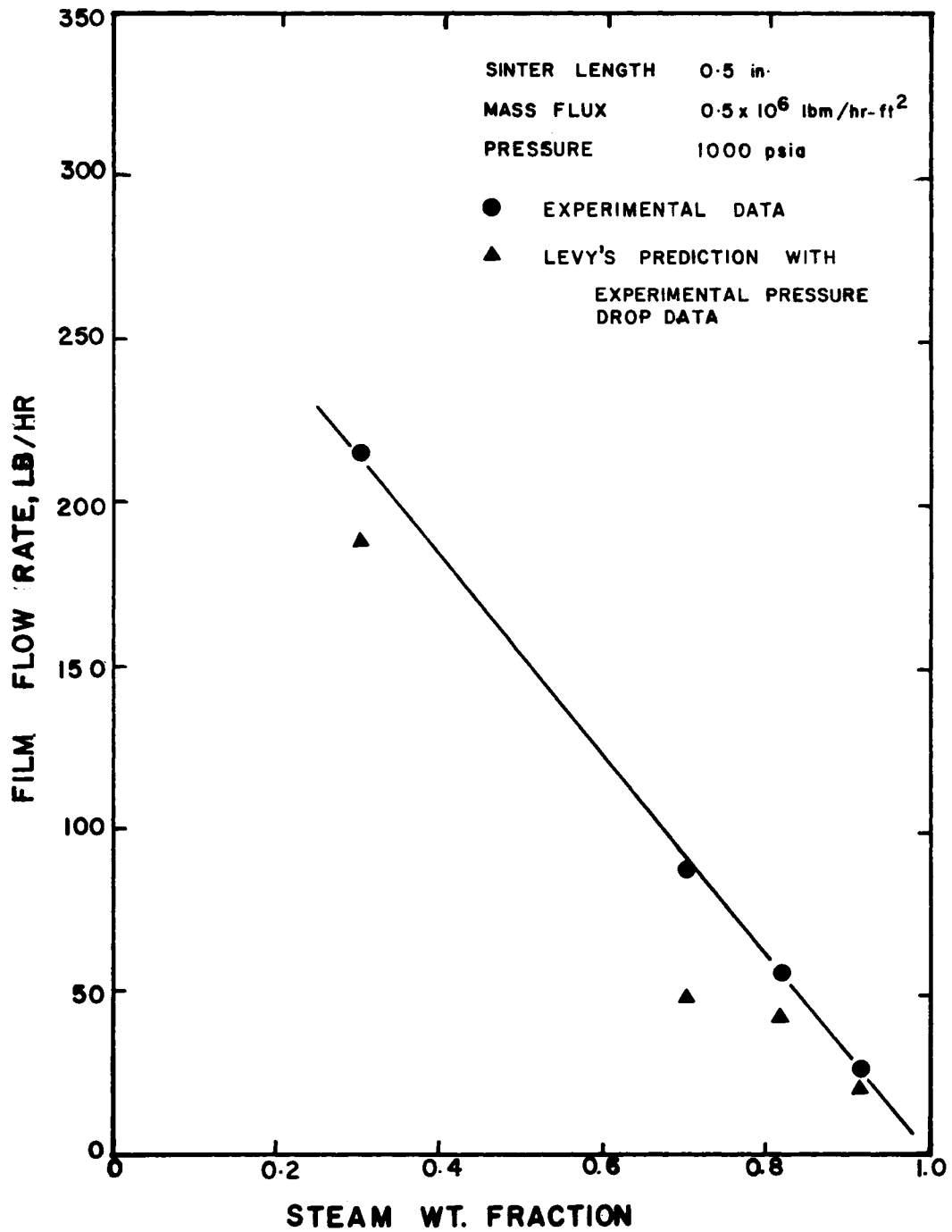


FIG. II VARIATION OF FILM FLOW RATES WITH QUALITY

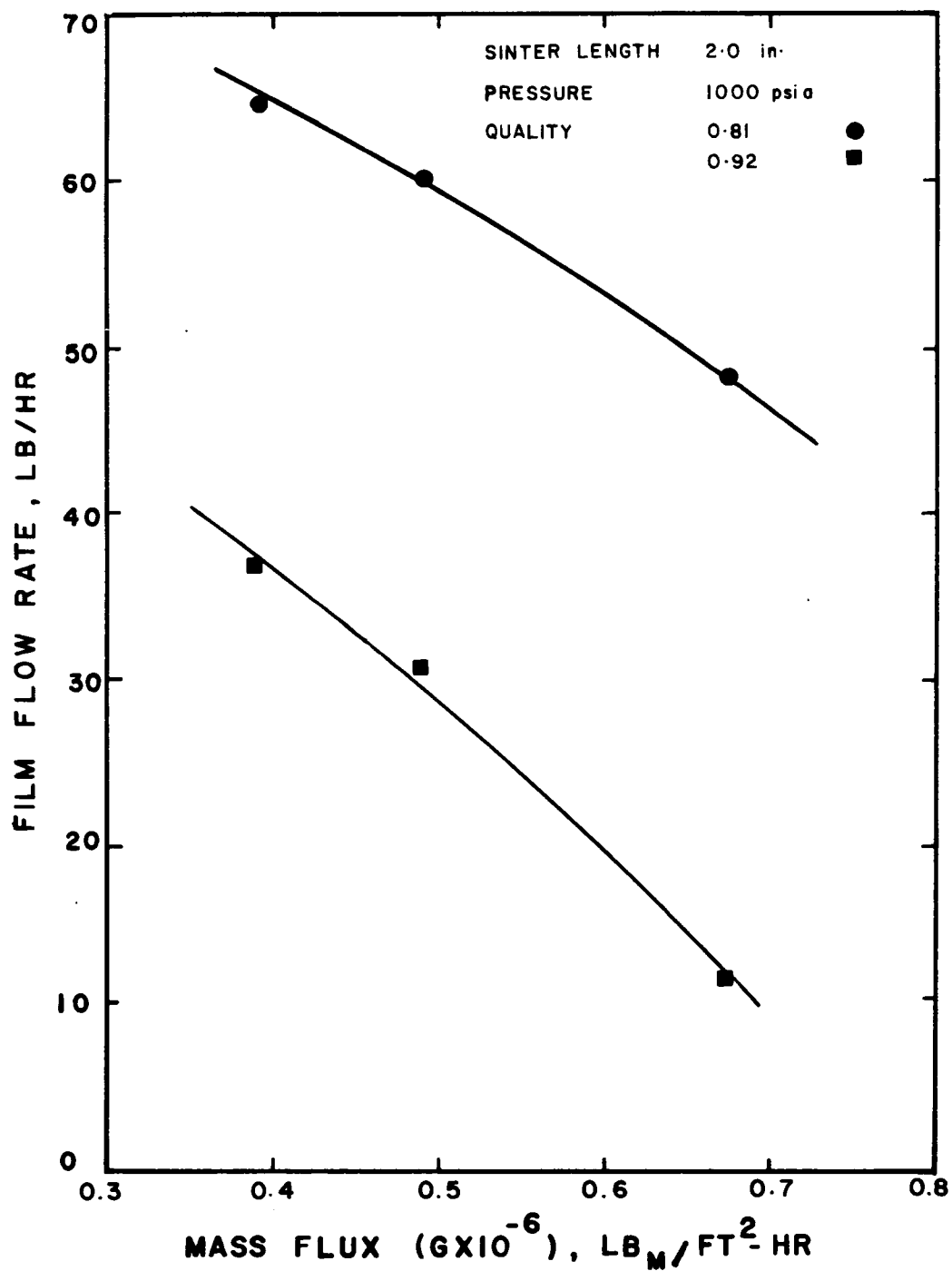


FIG.12. VARIATION OF FILM FLOW RATES WITH MASS FLUX.

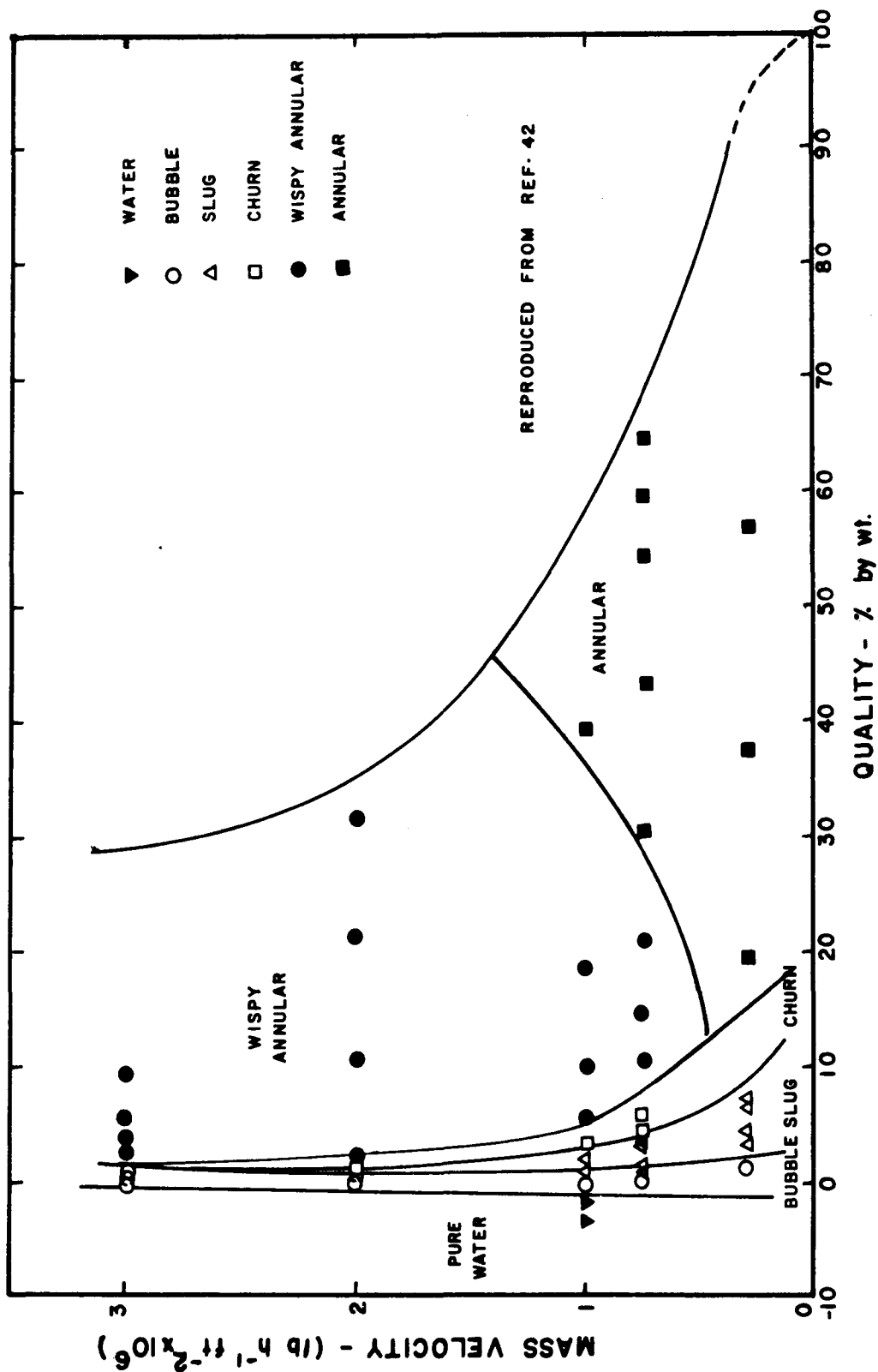


FIG.13 FLOW PATTERN DIAGRAM FOR STEAM / WATER FLOW AT 1000 P.S.I.A.

the flow regime presumably approaches churn flow. The flow-regime at a total mass flux of 0.5×10^6 lbm/hr.ft² and quality of 0.3 is probably on the transition line between "wispy annular" and annular flow. Churn flow is characterized by an unstable slug flow in which slugs of liquid break and the gas bubbles are unstable. In "wispy annular" flow, as defined in reference (42), the entrained phase appears to flow in large agglomerates while a liquid film moves on the tube wall. In both churn and wispy annular flow, the liquid flowing on the tube wall is less than the corresponding case of annular flow where the entrained phase is broken up into small droplets.

C. Effects of Sinter Length

One of the major objectives of the present study was to investigate the effect of sinter length on the liquid film extraction rates under similar conditions of total mass flux and quality. For the same flow conditions i.e. constant steam quality and total mass flux, experimental liquid film flow rates have been plotted against sinter lengths in Figure 14. It is observed that different film flow rates are obtained by use of various lengths of sinter. The testing of any theoretical model for the prediction of liquid film flow rate with experimental data can thus be greatly influenced by the sinter used to extract the film.

However, some of the experimental data show a trend contrary to the expected physical behaviour of the

phenomena under consideration. One would expect that the effect of employing a longer sinter, if any, would be to capture additional liquid from the core. Thus a 2-inch sinter might show higher film flows than the actual. On the other hand, crests of high-amplitude roll waves could miss the 1/2-inch sinter. Therefore a shorter sinter would extract lower film flows than a larger one. Figure 14 shows that film flow rates obtained with 1-inch sinter were actually higher than the corresponding figures obtained with 2-inch sinter.

During the experimental runs, it was noticed that the sinters became quite dark in colour after use, indicating oxidation. It is suspected that the 2-inch sinter became partially plugged due to oxidation. The 2-inch sinter was in the loop for over 35 days while the shorter sinters were there for less than seven days. The 1- and 1/2-inch sinters were weighed before putting them in the extractor section and again after use. The weight gains were 0.0473 gm for the one inch unit and 0.0329 gm for the one-half inch unit. The 2-inch sinter was not weighed before putting it in the extractor section. An accurate determination of weight gain for this sinter is not possible.

An attempt was made, by statistical methods, to estimate the weight of the two inch sinter before installation (47). Eight unused two inch sinters were found to have a mean weight of 43.1850 gm with a standard deviation of 0.1266 gm.

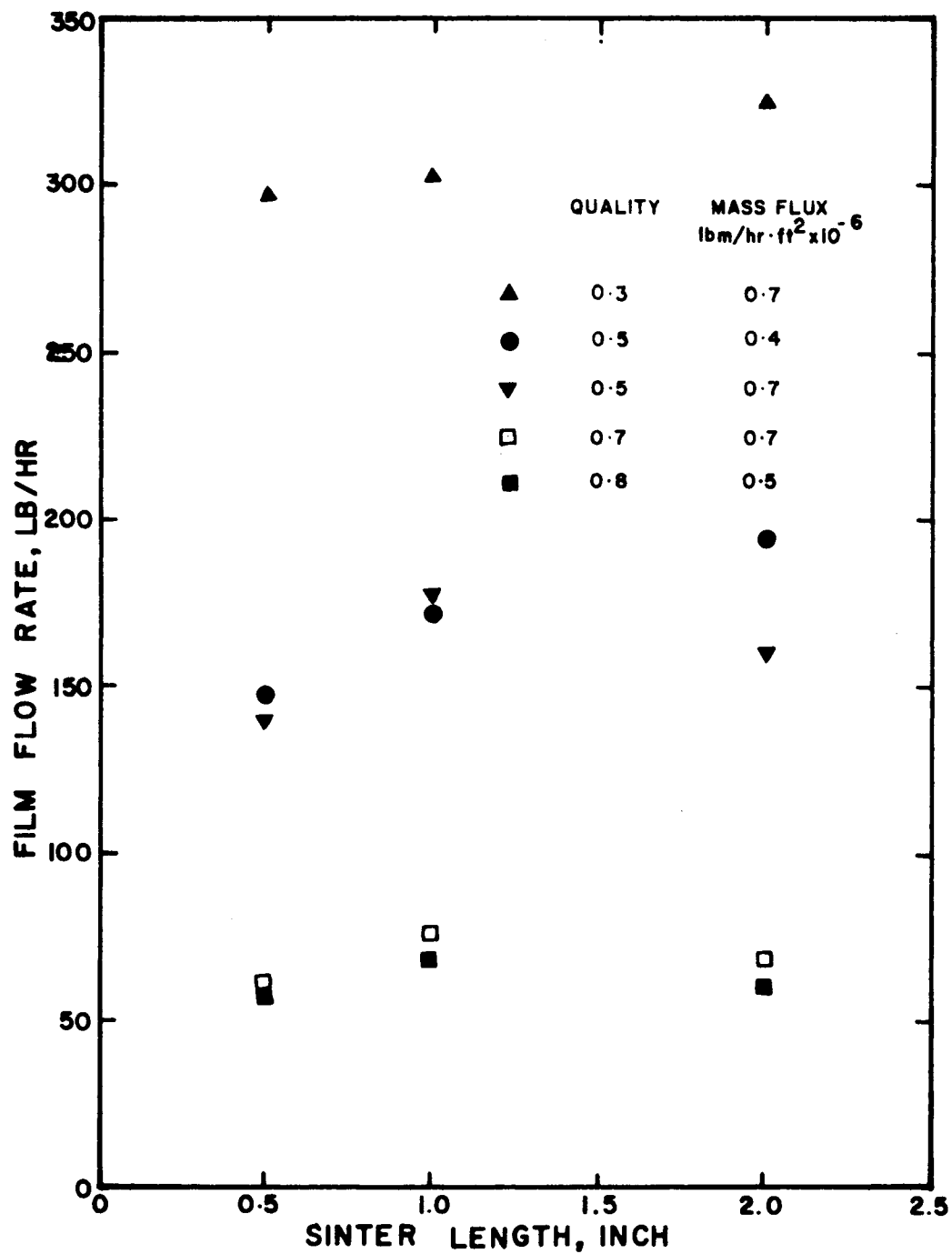


FIG.14 VARIATION OF FILM FLOW RATES WITH SINTER LENGTH

From careful measurements of the used sinter, it was estimated that between 2.294% and 2.347% of total volume of the raw sinter was removed by machining the chamber on either end. Therefore one would expect the mean weight of the population of machined two inch sinter to be between 42.1714 and 42.1943 gm. The standard deviation of this population can probably be assumed to be the same, namely 0.1266 gm.

Now assuming that a t-distribution adequately describes this sample, at the 95% confidence level with 7 degrees of freedom, the t statistic is 2.365. One would then expect, with 95% confidence that the true initial weight of the specimen was within 2.365 times the standard deviation of the true mean weight of the population of machined sinters. Allowing for the uncertainty of measurement previously described the 95% confidence estimate of the true initial weight, W , of the sinter becomes $41.8720 \text{ gm} < W < 42.4937 \text{ gm}$.

The actual measured weight of the sinter after removal from the test section was 42.7304 gm. It would appear then that with about 95% confidence, we can state that the weight gained, W_g , by the sinter during use was $0.2367 \text{ gm} < W_g < 0.8584 \text{ gm}$. This is quite large in comparison with the known weight gains of the shorter sinters.

It was suggested that, if in fact these sinters had collected foreign matter, it might be possible to remove some or all of this by ultrasonic cleaning. The three used sinters plus an unused two inch control specimen were

subjected to ultrasonic cleaning in acetone for a period of 3/4 hour, dried in air over-night and then oven dried at 225°F for 2 1/2 hours. The control specimen registered a weight gain of 0.0004 gm, while the 2-, 1- and 1/2-inch specimens had losses of 0.0050 gm, 0.0078 gm and 0.0006 gm respectively.

In view of the above results, it is reasonable to conclude that most of the weight gain which occurred was due to oxide formation. It is difficult to ascertain the effect of this partial clogging on the extractive properties of the sinter with any degree of confidence. Most probably it will extract lower film flow. It is suggested that different sinter grades should be used to look more deeply into this problem.

D. Comparison with Levy's Model

Experimental liquid film flow rates were compared with the theoretical predictions by Levy's (1) analytical model. The value of y_+ , the dimensionless Reynolds number based on the friction velocity, was more than 30 for all runs, thus indicating that Levy's analysis is applicable. A sample calculation is given in Appendix III.

The comparison between the measured values and the theoretical predictions for film flow rates is shown in Figure 15 for all the three sinter lengths. It is observed that the film flow rates as predicted by Levy's analysis were consistently lower than the experimentally observed

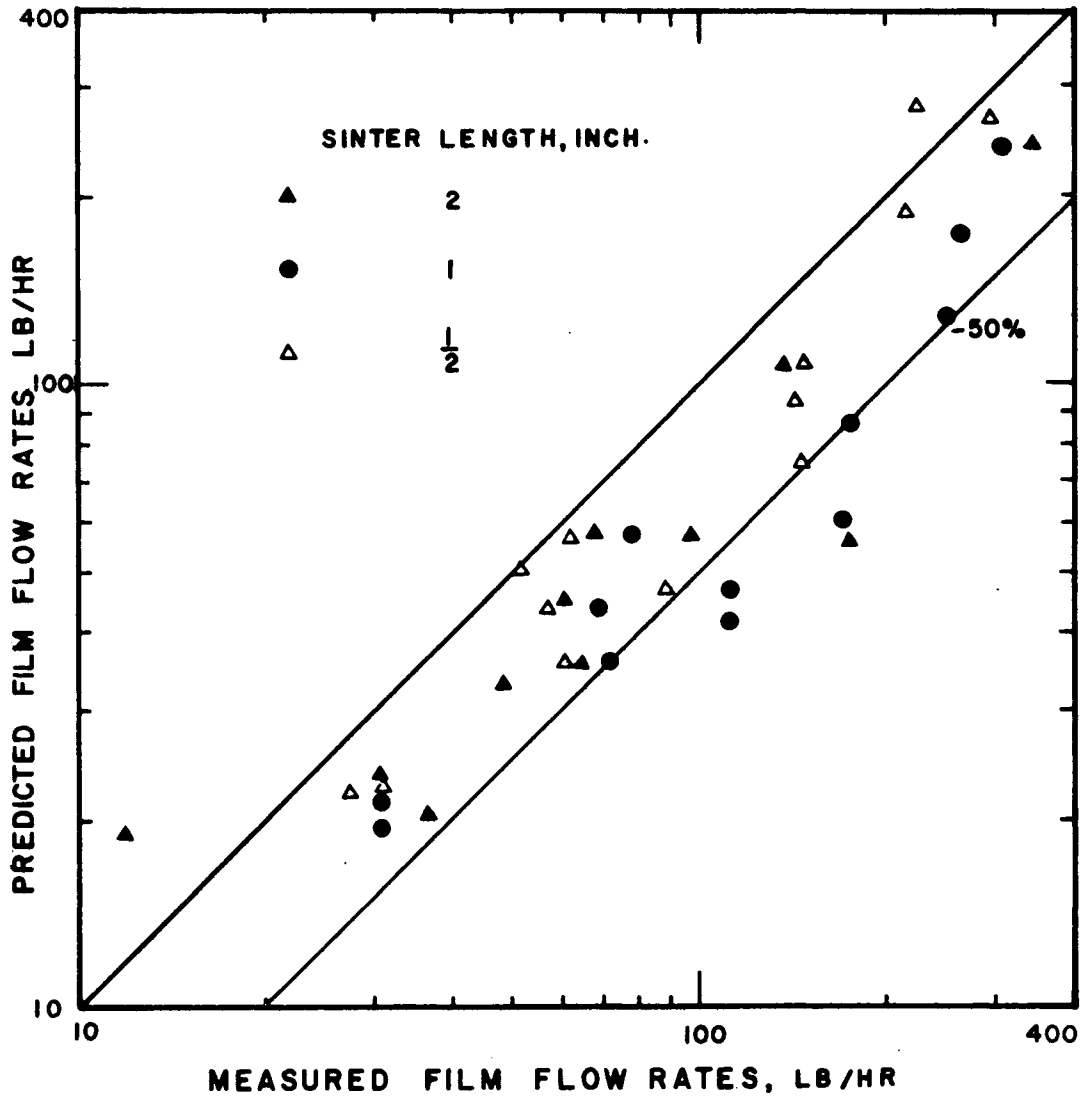


FIG.15 COMPARISON OF LEVY'S MODEL WITH EXPERIMENTAL DATA.

values. The deviation was, in general, less than 50%.

Appendix II of results shows one important trend. For the same values of total mass flux and quality, the film flow rates obtained by the use of one-half inch sinter show much better agreement with predictions by Levy's model as compared to data obtained with larger sinters. The Student's t-test was applied to the data to compare the relative performance of the three sinters vis-a-vis with predictions by Levy's model. The results obtained are detailed in Table 5.2.

TABLE 5.2

RELATIVE PERFORMANCE OF SINTERS

Comparison of Experimental Data with Levy's model by t-test

Sinter Length in.	No. of data points	Degrees of freedom	t	Level of significance
2	12	22	1.001	0.33
1	12	22	1.758	0.10
1/2	11	20	0.766	0.45

It should be noted that the last column in the above table gives the level at which the value of t becomes significant. The analysis shows that agreement of experimental data with Levy's model is the closest for one-half inch sinter. Poorer agreement of data obtained with the one-inch

sinter is shown by this analysis. However, this may not be the true indication of the performance of the sinter. As mentioned earlier, the two-inch sinter might have been partially clogged due to oxidation. Experimental results show that extraction rates obtained with the two-inch sinter for a major portion of the data are actually lower than the corresponding figures obtained with the one-inch sinter. It is believed that the flows would have been higher if the sinter had not been clogged and for this reason, the experimental data with the 2-inch sinter indicates better agreement with Levy's model as compared to the one-inch unit.

In view of the above reasoning, it can be stated that film flow rates obtained by one-half inch sinter are probably nearer to the actual film flow rates on the tube wall. The larger sinters are possibly capturing liquid from the core also. The liquid film flow rates as obtained with these sinters are, therefore, higher than the actual flow rates.

E. Comparison with Minh's Model

Experimental film flow rates have been plotted against predicted values calculated from the model proposed by Minh and Huyghe (2) in Figure 16. It is seen that the agreement between the two is very poor, the deviation being as high as +200%. The model as suggested is applicable only for air-water mixtures at low pressures. Apparently it cannot be applied to steam-water mixtures at high pressures without some modification.

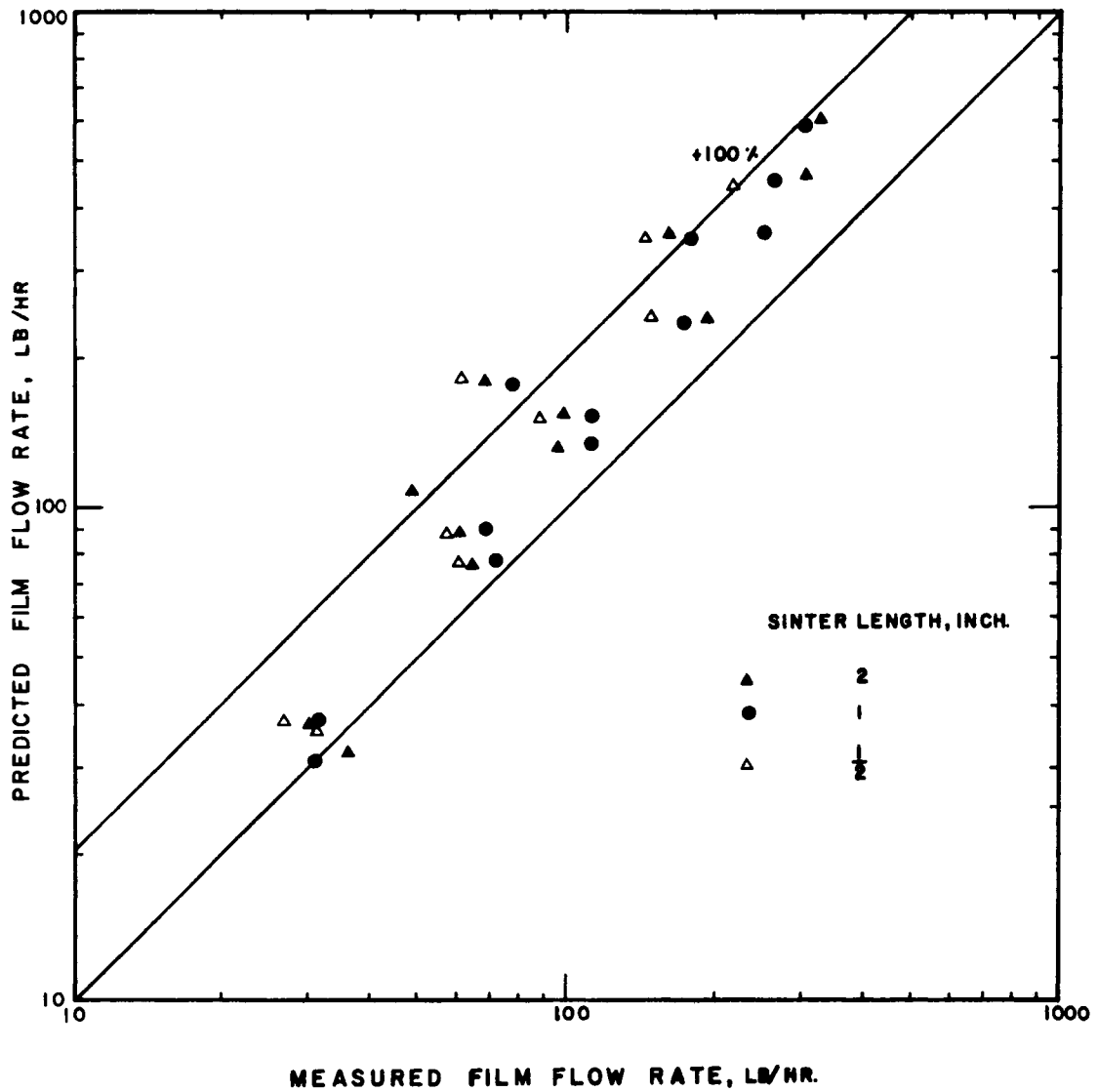


FIG.16 COMPARISON OF MINH'S MODEL WITH EXPERIMENTAL DATA.

VI. CONCLUSIONS

Experimental measurements have been made of the liquid film flow rates for steam-water mixtures flowing in a vertical test section at high pressures. In order to extract the liquid film on the wall, sinters of various lengths were employed; a technique used previously by the Harwell group (3,4,5). Marked effect of sinter length on the extracted liquid film flow rates has been demonstrated.

Qualitatively, the variation of liquid film flow rates with quality and total mass flux was found to be physically consistent. The experimental film flow rates have been compared with the theoretical predictions of Levy (1) for annular flow. It has been shown that the model predicts consistently lower film flow rates, the deviation being as high as 64%. Agreement of theoretical predictions from the model with the experimental data obtained by use of 1/2-in sinter was much better than in case of longer sinters. It is suggested that film flow rates obtained with shorter sinters are probably closer to the actual film flow rates, with the longer sinters extracting additional liquid from the core. The experimental results were also compared with the semi-empirical model of Minh (2). Deviations of up to +200% were noticed. The model is not suitable for use in steam-water flows at high pressures without some modification.

Experimental pressure gradients were compared with theoretical predictions of Martinelli and Nelson (21) and Owen (16). Owen's model gave reasonably good agreement with the observed values.

It is recommended that more experimental data should be taken to study the effects of pressure and sinter grades on the liquid film flow rates.

NOMENCLATURE

Dimensions are given in terms of mass (M), length (L), time (t) and temperature (T).

A	Cross-sectional area of channel	L^2
D	Diameter	L
f	Friction Factor	
G	Mass Flux	M/tL^2
g_c	Gravitational conversion factor	
$\frac{\Delta P}{\Delta L}$	Pressure drop per unit length	M/L^2t^2
P	Pressure	M/Lt^2
R_l	Fraction of pipe filled with liquid	
R_g	Fraction of pipe filled with gas	
\bar{V}	Average velocity	L/t
\bar{v}	Average specific volume	L^3/M
v	Specific volume	L^3/M
W	Mass flow rate	M/t
x	Quality $\left(\frac{\text{steam flow rate}}{\text{total flow rate}}\right)$	
X	Two-phase flow modulus defined by Lockhart and Martinelli	

Greek Symbols

ρ	Density	M/L^3
--------	---------	---------

μ	Viscosity	M/Lt
Φ	Function of X utilized in calculating two-phase pressure drop	

Subscripts

e	elevation
f	friction
g	gas or steam phase
l	liquid or water phase
m	momentum
s	static
TP	two-phase
T	total

REFERENCES

1. Levy, S., Prediction of Two-Phase Annular Flow with Liquid Entrainment, Int. J. Heat Mass Transfer, 9, pp. 171-188, (1966).
2. Minh, T.Q. and J.D. Huyghe, Some Hydrodynamical Aspects of Annular Dispersed Flow: Entrainment and Film Thickness, Symposium on Two-Phase Flow, University of Exeter, 1, pp. C201-C212, (1965).
3. Hewitt, G.F., H.A. Kearsley, P.M.C. Lacey and D.J. Pulling, Burn-out and Nucleation in Climbing Film Flow, AERE-R 4374, (1963).
4. Staniforth, R., G.F. Stevens and R.W. Wood, An Experimental Investigation into the Relationship between Burn-out and Film Flow-rate in a Uniformly Heated Round Tube, AEW-R 430, (1965).
5. Hewitt, G.F., H.A. Kearsley, P.M.C. Lacey and D.J. Pulling, Burn-out and Film Flow in the Evaporation of Water in Tubes, AERE-R 4864, (1965).
6. Hewitt, G.F. and P.M.C. Lacey, The Breakdown of the Liquid Film in Annular Two-Phase Flow, AERE-R 4303, (August, 1963).
7. Goldman, K., H. Firstenberg and C. Lombardi, Burnout in turbulent flow - a droplet diffusion model, J. Heat Transfer, 83, p. 158, (1961).
8. Kirby, G.J., Burnout in Climbing Film Two Phase Flow, AEW-R 470, (March, 1966).
9. Isbin, H.S., R. Vanderwater, H. Fauske and S. Singh, A Model for correlating two phase, steam water, burnout heat transfer fluxes, J. Heat Transfer, 83, p. 149, (1961).
10. Becker, K.M. and P. Persson, An analysis of burnout conditions for flow of boiling water in a vertical round duct, J. Heat Transfer, 86, p. 515, (1964).
11. Grace, J.M., The Mechanism of burnout in initially subcooled forced convection systems, TID-19845.

REFERENCES (contd.)

12. Grace, T.M. and H.S. Isbin, Comment on paper by Becker, ASME Journal of Heat Transfer, p. 524, (Nov., 1964).
13. Collier, J.G. and G.F. Hewitt, Measurement of Liquid Entrainment, British Chem. Engg., 11, pp. 1375-1379, (1966).
14. Gill, L.E. and G.F. Hewitt, Further Data on the Upwards Annular Flow of Air-Water Mixtures, AERE-R 3935, (April, 1962).
15. Cousins, L.B., W.H. Denton and G.F. Hewitt, Liquid Mass Transfer in Annular Two-Phase Flow, AERE-R 4926, (1965).
16. Owens, W.L., Two-Phase Pressure Gradient, Paper No. 41, International Heat Transfer Conference, (1961).
17. McAdams, W.H., W.K. Woods and L.C. Heroman, Vaporization inside Horizontal Tubes - II - Benzene - Oil Mixtures, Trans. A.S.M.E. 64, pp. 193, (1942).
18. Collier, J.G., Heat Transfer and Fluid Dynamic Research as applied to Fog Cooled Power Reactors, AECL-1631, (June, 1962).
19. Dukler, A.E., Moye Wicks and R.G. Cleveland, Frictional Pressure Drop in Two-Phase Flow: A. A Comparison of Existing Correlations for Pressure Loss and Holdup, A.I. Ch.E. Journal, 10, pp. 38-43, (1964).
20. Lockhart, R.W. and R.C. Martinelli, Proposed Correlation of Data for Isothermal Two-Phase, Two-Component Flow in Pipes, Chem. Engg. Prog., 45, 1, pp. 39-48 (1949).
21. Martinelli, R.C. and D.B. Nelson, Prediction of Pressure Drop During Forced-Circulation Boiling of Water, Trans. A.S.M.E., pp. 695-702, (Aug. 1948).
22. Martinelli, R.C., L.M.K. Boetler, T.H.M. Taylor, E.G. Thomsen and E.H. Morrin, Isothermal Pressure Drop for Two-Phase Two-Component Flow in a Horizontal Pipe, Trans. A.S.M.E., pp. 139-151 (Feb., 1944).
23. Martinelli, R.C., J.A. Putnam and R.W. Lockhart, Two-Phase, Two-Component Flow in the Viscous Region, Trans. A.I. Ch.E., 42, 4, pp. 651-705, (1946).

REFERENCES (Contd.)

24. Isbin, H.S., R.H. Moen, R.O. Wickey, D.R. Mosher and H.C. Larson, Two-Phase Steam-Water Pressure Drops, Nuclear Engineering, Chem. Engg. Prog. Sump. Series No. 23, 55, pp. 75-84, (1958).
25. Sher, N.C., Estimation of Boiling and Non-Boiling Pressure Drop in Rectangular Channels at 2000 psia, WAPD-TH-300 (1957).
26. Hoglund, B.M., Two-Phase Pressure Drop in a Natural Circulation Boiling Channel, ANL-5760, (1961).
27. Jones, A.B. and D.G. Dight, Hydrodynamic Stability of a Boiling Channel, Part I, KAPL-2170, (1961).
28. Hewitt, G.F., R.D. King and P.C. Lovegrove, Liquid film and Pressure Drop Studies, Chem. and Process Engg., pp. 191-200, (April, 1964).
29. Lacey, P.M.C., G.F. Hewitt and J.G. Collier, Climbing Film Flow, AERE-R 3962, (January, 1962).
30. Wicks, M. and A.E. Dukler, Entrainment and Pressure Drop in Concurrent Gas-Liquid Flow, A.I.Ch.E. J., 6, No. 3, p. 463, (1960).
31. Gill, L.E. Sampling Probe Studies of the gas core in Annular Two-Phase Flow, AERE-R 3954.
32. Wallis, G.B. The onset of Droplet Entrainment in Annular Gas-Liquid Flow, 62-GL-127.
33. Charvonia, D.A., A Review of the Published Literature Pertaining to the Annular, Two-Phase Flow of Liquid and Gaseous Media in a Pipe, Purdue Univ. Tech. Report, PUR-32-R, (Dec. 1958).
34. Bennett, J.A.R., Two Phase Flow in Gas Liquid Systems-A Literature Survey, AERE-R 2497, (March, 1958).
35. Anderson, G.H. and B.G. Mantzouranis, Two-Phase flow phenomena-I, Chem. Eng. Sci. 12, pp. 109-126, (1960).
36. Calvert, S. and B. Williams, Upwards Cocurrent Annular Flow of Air and Water in Smooth Tubes, A.I.Ch.E.J., 1, No. 1, pp. 78-86, (1955).

REFERENCES (Contd.)

37. Dukler, A.E., Fluid Mechanics and heat transfer in Vertical Falling Film systems, ASME-AIChE Third National Heat Transfer Conference, (August, 1959).
38. Hewitt, G.G., Analysis of Annular Two-Phase Flow, AERE-R 3680, (1961).
39. Adorni, N., I. Casagrande, L. Cravarolo, A. Hassid and M. Silvestri, Experimental data on two-phase adiabatic flow, CISE-R 35, (1961).
40. Baker, James L.L., Flow-Regime Transitions at Elevated Pressures in Vertical Two-Phase Flow, ANL-7093, (1965).
41. Griffith, P., The Slug-Annular Flow Regime Transition at Elevated Pressure, ANL-6796, (1963).
42. Bennett, A.W., G.F. Hewitt, H. A. Kearsey, R.K.F. Keays and P.M.C. Lacey, Flow Visualisation Studies of Boiling at High Pressure, AERE-R 4874, (March, 1965).
43. Tippetts, F.E., Critical Heat Flux and flow pattern Characteristics of High Pressure Boiling Water in Forced Convection, GEAP-3766.
44. Hostler, E.R., Visual study of Boiling at High Pressure, WAPD-T1566.
45. Wallis, G.B., The Transition from Flooding to Upwards Cocurrent Annular Flow in a Vertical Pipe, AEEW-R 142, (1962).
46. Hewitt, G.F., Flooding and Associated Phenomena in Falling Film Flow in a Tube, AERE-R 4022, (1963).
47. Crago, W.A., Atomic Energy of Canada Ltd., Chalk River, personal communication.

APPENDIX I

Calculation of Liquid Flow Rate from a Mixture of Liquid and Vapour

Temperature and pressure on the inside of the sinter should be accurately known.

Let

W_e : Mass flow rate of extract

W_s : Mass flow rate of steam removed

W_w : Mass flow rate of liquid

H_s : Enthalpy of steam at the sinter

H_w : Enthalpy of liquid at the sinter

T_7 : Temperature of extract at outlet of the cooler

W_c : Coolant flow rate

T_8 : Inlet temperature of coolant

T_9 : Outlet temperature of coolant

H_1 : Heat losses to the atmosphere

Heat lost by extract (water + steam) =

$$(W_e - W_w) H_s + W_w H_w - W_e (T_7 - 32) C_p$$

$$\text{Heat absorbed by coolant} = W_c (T_9 - T_8) C_p$$

$$\text{Heat lost} = \text{Heat absorbed} + H_1$$

$$W_w = \frac{W_e H_s - W_e (T_7 - 32) C_p - W_c (T_9 - T_8) C_p - H_1}{H_s - H_w}$$

All other quantities being known, W_w , the liquid film flow rate can be calculated. Heat losses to the atmosphere, H_1 , were estimated to be 3073 Btu/hr.

APPENDIX II

Liquid Film Flow Rates at 1000 psia

Run	Sinter Length in.	Quality	Total mass flux $\frac{\text{lbm}}{\text{hr} \cdot \text{ft}^2} \times 10^{-6}$	Pressure Gradient, psi/foot			Liquid Film Flow Rate, lb/hr				Remarks	
				Exptl	Owen's Model	M and N Model	Exptl	Levy's Model	% Deviation	Minh's Model		
1	2	0.289	0.515	0.273	0.268	0.483	0.436	302.0	175.6	-	459.8	Semi-annular flow
2	1	0.296	0.514	0.275	0.270	0.483	0.436	262.0	175.6	-33.0	452.9	Semi-annular flow
3	1/2	0.305	0.507	0.274	0.269	0.485	0.434	215.1	189.4	-12.0	439.7	Semi-annular flow
4	2	0.278	0.708	0.455	0.449	-	-	325.0	-	-	599.0	
5	1	0.291	0.712	0.474	0.467	0.759	0.753	304.0	241.8	-20.4	582.9	
6	1/2	0.288	0.707	0.465	0.458	0.748	0.738	297.0	267.4	-10.0	584.6	
7	2	0.490	0.399	0.247	0.239	-	-	194.0	-	-	243.1	
8	1	0.509	0.404	0.259	0.251	0.469	0.396	171.0	60.9	-64.3	234.8	
9	1/2	0.495	0.404	0.254	0.246	0.461	0.389	147.5	75.1	-49.0	242.6	
10	2	0.492	0.715	0.712	0.698	-	-	160.0	-	-	357.1	
11	1	0.498	0.704	0.699	0.685	1.077	1.061	176.5	87.4	-50.5	348.1	
12	1/2	0.500	0.709	0.712	0.698	1.098	1.081	144.0	94.0	-34.7	347.7	
13	2	0.599	0.398	0.335	0.309	0.558	0.465	96.0	57.4	-40.2	131.3	
14	1	0.594	0.399	0.309	0.321	0.558	0.466	112.0	41.7	-62.8	133.8	
15	2	0.704	0.692	0.781	0.910	1.337	1.310	68.0	57.6	-15.2	179.8	
16	1	0.712	0.701	0.792	0.943	1.381	1.355	77.0	57.9	-24.7	174.9	
17	1/2	0.701	0.690	0.765	0.903	1.381	1.355	62.0	56.7	-8.5	181.6	
18	2	0.689	0.483	0.453	0.439	-	-	98.5	-	-	154.8	
19	1	0.697	0.498	0.448	0.470	0.799	0.701	112.7	47.3	-58.0	153.1	
20	1/2	0.703	0.499	0.455	0.491	0.808	0.709	88.0	47.0	-46.5	150.0	
21	2	0.814	0.389	0.346	0.350	0.594	0.492	64.5	35.8	-44.5	76.5	
22	1	0.813	0.396	0.352	0.360	0.610	0.507	72.2	35.8	-50.4	77.9	
23	1/2	0.815	0.396	0.358	0.360	0.609	0.506	61.0	36.6	-40.0	76.9	
24	2	0.798	0.198	0.107	0.100	-	-	51.8	-	-	50.0	Semi-annular flow
25	1	0.794	0.197	0.106	0.100	-	-	58.7	-	-	50.9	Semi-annular flow
26	1/2	0.799	0.201	0.113	0.110	0.201	-	46.8	26.2	-43.9	50.7	Semi-annular flow
27	2	0.814	0.490	0.524	0.537	0.865	0.754	60.3	45.0	-25.3	88.1	
28	1	0.811	0.491	0.513	0.538	0.866	0.755	68.0	44.3	-34.8	89.8	
29	1/2	0.814	0.480	0.497	0.516	0.836	0.724	57.2	43.5	-23.9	87.2	
30	2	0.918	0.391	0.368	0.390	0.375	0.533	36.7	21.0	-42.7	32.5	
31	1	0.924	0.404	0.387	0.418	0.684	0.568	30.7	19.5	-36.5	30.7	
32	1/2	0.910	0.381	0.354	0.370	0.615	0.506	31.0	22.9	-26.2	35.1	
33	2	0.920	0.489	0.555	0.575	0.933	0.811	30.8	23.6	-23.3	36.1	
34	1	0.919	0.493	0.552	0.605	0.947	0.825	30.7	21.4	-30.1	36.8	

APPENDIX II (Contd.)

Liquid Film Flow Rates at 1000 psia

Run	Sinter Quality	Total mass flux $\frac{\text{lbm}}{\text{sq. ft.} \times 10^6}$	Pressure Gradient, psi/foot				Liquid Film Flow Rate, lb/hr.				Remarks	
			Exptl	Owen's Model	M. and N. Model		Exptl	Levy's Model	% Deviation	Minh's Model		
				f_{TP-f1}	f_{TP-f}	With Jones's Corr. Factor						Without Jones's Corr. Factor
35	1/2	0.485	0.536	0.585	0.565	0.919	0.798	27.2	21.8	-19.8	37.2	
36	1	0.407	0.172	0.192	0.188	0.352	0.304	251.0	129.0	-48.4	36.0	
37	2	0.199	0.117	0.093	0.089	0.178	0.144	94.3	25.4	-73.0	100.2	Semi-annular flow
38	2	0.388	0.109	0.083	0.081	0.159	0.134	87.7	107.4	22.5	142.5	Semi-annular flow
39	2	0.199	0.111	0.087	0.084	0.168	0.138	116.0	54.7	-52.8	123.5	Semi-annular flow
40	2	0.704	0.119	0.100	0.095	0.187	0.148	76.4	14.6	-80.7	74.7	Semi-annular flow
41	2	0.926	0.931	1.106	1.077	1.551	-	11.8	19.2	+63	39.4	
42	2	0.814	0.845	0.991	0.966	1.423	1.388	48.0	33.0	-31	105.3	

Liquid Film Flow Rates at 1200 psia

43	2	0.284	0.210	0.243	0.239	0.418	0.372	280.5	198.8	-29.0	468.8	Semi-annular flow
44	2	0.298	0.313	0.410	0.405	0.646	0.635	342.0	244.5	-28.5	588.0	
45	2	0.489	0.456	0.575	0.564	0.881	0.864	136.0	107.2	-21.1	371.1	
46	2	0.488	0.101	0.211	0.206	0.387	0.319	174.0	56.0	-67.8	248.6	
47	1/2	0.270	0.304	0.286	0.281	0.607	0.597	222.0	278.0	25.2	623.7	
48	1/2	0.476	0.418	0.533	0.523	0.830	0.804	148.0	109.3	-26.0	377.1	
49	1/2	0.707	0.604	0.731	0.715	1.087	1.05	51.5	50.3	-2.3	184.2	

APPENDIX III

Sample Calculation for Theoretical Liquid Film Flow Rate using Levy's (1) Model

All references in the following treatment are from Levy's original paper.

Quality of steam	=	0.698
Total mass flux, G_T	=	0.398×10^6 lbm/hr.ft ²
Pressure	=	1000 psia
Diameter of test section	=	0.04108 ft
X-sectional area	=	1.3256×10^{-3} sq ft
Density of water	=	46.29 lbm/cu ft
Density of steam	=	2.24 lbm/cu ft
Viscosity of water	=	0.241 lbm/hr.ft
$(\Delta P/\Delta L)$, EXPTL	=	48.29 lb _f /ft ²
Steam mass flux, G_g	=	(Total mass flux) (Quality)
	=	0.278×10^6 lbm/hr.ft ²
$R = (\rho_l/\rho_g)^{1/3}$	=	2.74

$$F(2t/D) = \sqrt{\frac{(-dp/dL)(D/4) g_c}{\rho_l}} \frac{\rho_g}{G_g} R \left(\frac{\rho_l}{\rho_g}\right)$$

$$= 0.0468$$

Plot of $F(2t/D)$ vs $(2t/D)$ in Figure 7 was curve-fitted to find $(2t/D)$ corresponding to any value of $F(2t/D)$.

For $F (2t/D) \geq 0.04$,

$$\begin{aligned} (2t/D) &= 0.870313 - 64.295 \times F (2t/D) + 1.794128 \times 10^3 \times \\ & \left[F (2t/D) \right]^2 - 2.34222 \times 10^4 \times \left[F (2t/D) \right]^3 + 1.469566 \times 10^5 \times \\ & \left[F (2t/D) \right]^4 - 3.54543 \times 10^5 \times \left[F (2t/D) \right]^5 \\ & = 0.0154 \end{aligned}$$

Therefore, thickness of liquid film = 0.000316 ft

$$\text{Wall shear stress, } \tau_w = \left[(-dp/dL) - \rho_1 (1 - a^2/b^2) \right] \frac{D}{4}$$

$$\text{where } a = D/2 - t$$

$$b = D/2$$

$$\tau_w = 0.4814$$

$$y^+ = t \sqrt{\frac{\tau_w g_c}{\rho_1 \mu_1}} \frac{\rho_1}{\mu_1}$$

$$= 126.3$$

$$F(y^+) = 3y^+ + 2.5 y^+ \ln y^+ - 64 \quad (\text{Eq. 15})$$

$$= 1844$$

$$\text{Liquid Film Flow Rate} = \frac{4 \mu_1 F(y^+) \cdot (\text{X - Sectional area})}{D}$$

$$= 57.4 \text{ lbm/hr}$$

VITA AUCTORIS

- 1940 Born in Gujranwala, Punjab, W. Pakistan.
- 1964 Graduated from Punjab University, Chandigarh, India, with the degree of B.Sc. in Chemical Engineering.
- 1965 Accepted into the Graduate School of University of Windsor as candidate for the degree of M.A.Sc. in Chemical Engineering.